DOE/PC/90364--T8

MAR 01 1994

M-1
2

Flue Gas Conditioning for Improved Particle Collection in Electrostatic Precipitators

Quarterly Technical Report
October 1-December 31, 1993

Contract No. DE-AC22-91PC90364

Prepared for:

U.S. Department of Energy

Pittsburgh Energy Technology Center
Pittsburgh, PA 15236

Project Officer: Mr. Thomas Brown

Prepared by
Michael D. Durham, Ph.D.
Kenneth E. Baldrey

ADA Technologies, Inc.
304 Inverness Way So.
Englewood, CO 80112
(303) 792-5615

ADA Report 4300-93-Q4

January 12, 1994

MASTER

DISTRIBUTION OF THIS DOCUMENT IS UNLIMITED

Program Objectives

The purpose of this research program is to identify and evaluate a variety of additives capable of increasing particle cohesion which could be used for improving collection efficiency in an ESP. A three-phase screening process will be used to provide the evaluation of many additives in a logical and cost-effective manner. The three step approach involves the following experimental setups:

1. Provide a preliminary screening in the laboratory by measuring the effects of various conditioning agents on reentrainment of flyash particles in an electric field operating at simulated flue gas conditions.
2. Evaluate the successful additives using a 100 acfm bench-scale ESP operating on actual flue gas.
3. Obtain the data required for scaling up the technology by testing the two or three most promising conditioning agents at the pilot scale.

The objectives of this program are addressed in ten tasks defined in the Management Plan. During the three months covered by this report, work was focused in Tasks 3 and 4.

Activities Completed During Current Reporting Period

Task 5. Testing at the CONSOL Coal Combustion Research Facilities

During the quarter, the initial pilot-scale testing of two additives was completed at CONSOL's research coal combustor. The results and conclusions from this test series and subsequent analysis of the data are presented in this report.

The pilot-scale test program extended for two weeks during September and October, 1993. Table 1 summarizes the conditions tested. During the tests, the research combustor was firing a medium-sulfur coal. The combustor had recently been retrofitted with low-NOx burners for a DOE Clean Coal test program. Operation of the low-NOx burners required a reduced flow rate in the combustor, resulting in lower flow and velocity in the ESP.

During the first week, a comprehensive baseline condition was tested, followed by initial screening runs for several additives. It was discovered that at the conditions tested, the flyash exhibited properties characteristic of a high-resistivity ash. In-situ measurements at the ESP inlet confirmed that the resistivity was in the 10^{10} - 10^{12} ohm-cm range. In addition, the ESP plate rappers were not able to remove ash buildup on the first section during normal operation. Power off rapping was periodically required to fully clean the plates; this is a clear indication of high-resistivity conditions.

Since the major benefit of ESP additives will be to reduce reentrainment at low to midrange resistivity, this operating condition was undesirable for performance testing. It was decided to continue the program with SO_3 conditioning of the flue gas to reduce particle resistivity. It was also decided to operate with two rather than three electrical fields energized. By reducing the ESP collection area, it was hoped that it would be easier to measure changes in ESP performance and to see an immediate indication of the effectiveness of SO_3 conditioning.

During the second test week, the ESP was reconfigured with two electrical sections energized and SO_3 conditioning at a rate of approximately 20 ppm. An additional baseline was run, followed by extended tests with two additives referred to in this report as Additive 'C' and Additive 'D'. The system was allowed to return to baseline at the conclusion of the tests.

Table 1. Test Conditions for ESP Additives Pilot-Scale Tests

Test Condition	Dates	Remarks
Week 1		
Baseline, 3 electrical fields energized	9/21 - 9/23/93	200 SCA, high-resistivity ash
Preliminary Additives Testing, begin SO_3 conditioning	9/23 - 9/24	Rapid screening of several additives
Week 2		
Baseline with SO_3 conditioning, 2 electrical fields energized	9/28 - 9/29	Reduced SCA, resistivity is 10^{10} - 10^{11} ohm-cm
Additive 'C' Injection, SO_3 Conditioning	9/29	Injection rate is 0.2% of total particulate
Additive 'D' Injection, SO_3 Conditioning	9/29 - 9/30	Injection rate is 0.2% of total particulate
Final Baseline Period	9/30 - 10/01	SO_3 Conditioning, same SCA

ESP Operating Conditions

The CONSOL research combustor and ESP are extensively instrumented and can be configured for a variety of operating conditions. For the baseline test, the electrical sections were combined to give a 3 field configuration. Gas velocity in the precipitator was 1.7 ft/sec, based on a measured inlet flow rate of 468 acfm. Specific collection area (SCA) at this condition was 204 ft^2/kacfm. The precipitator was operated in a current limited mode throughout the test period. For the second week of testing, two electrical sections were energized. Gas velocity and flow rate in the precipitator were unchanged from the baseline. SCA was 129 ft^2/kacfm.

Voltage, current, and power for each electrical section were monitored continuously. Particulate buildup on the plates was also monitored via load cell transducers. Opacity was monitored at the ESP outlet, using a transmissometer mounted along a straight section of the outlet duct, for improved resolution. System temperatures, flow rates, and gas constituents exiting the boiler were also monitored. Table 2 lists typical measured concentrations of important gas constituents at the combustor outlet. Appendix A to this report includes a series of plots of continuous ESP data taken throughout the test program, superimposed on a timeline of the test. These plots are constructed from 5-minute average values for each parameter.

Table 2. Typical Flue Gas Concentrations at the Combustor Outlet

Gas Constituent	Range
Oxygen	3.5 - 4.5% by volume
Carbon Dioxide	10 - 14% by volume
Sulfur Dioxide	1,000 - 1,500 ppmv
Carbon Monoxide	9 - 15 ppmv
NO_x as NO	300 - 450 ppmv

Additive Injection

Additive was introduced to the flue gas via a fine spray nozzle oriented upstream in the duct, at a point downstream of the combustor convection zone outlet and 60 ft. upstream of the ESP. The ducting has several sharp bends between the spray point and the ESP, which ensured good contact between additive and entrained particulate prior to the ESP. Duct velocity was 22 - 25 ft/sec immediately upstream of the ESP inlet cone.

The spray nozzle had been previously calibrated at ADA's Nozzle Test Facility and was found to produce an extremely fine mist of approximately 10 μm droplet size. Injection rate was controlled using a peristaltic pump with pressure regulated compressed air. Actual consumption of additive solution was also monitored gravimetrically.

Injection rate was 36 cc/minute of a 0.065% by weight solution in water for both Additive 'C' and Additive 'D'. This gave a total additive injection of 0.003 lbs/hr, which was approximately 0.2% by weight of the total flue-gas particulate.

During the first week of testing, several other additives were briefly injected at rates of up to 1% by weight of total particulate. None of the tests showed a marked effect on ESP performance, as measured by outlet opacity and ADA's Insitec PCSV-E laser particle-sizing instrument.

Particle Resistivity

In-situ flyash resistivity measurements were made at the inlet duct to the CONSOL ESP using the ADA field resistivity instrument. Sampling was conducted isokinetically from the duct center at a sample port immediately prior to the ESP inlet expansion section. Dust samples of approximately 0.5 millimeters thickness were precipitated in 60 minutes during baseline without SO_3 conditioning. Dust layer thickness for the same sample time increased to approximately 0.6 - 0.8 millimeter during SO_3 conditioning, but no dramatic increase in precipitation rate was observed. Measurements were performed at the duct inlet gas temperature, nominally 300 ^{o}F. Resistivity ranged from 10^{10} to nearly 10^{12} ohm-cm for the initial baseline. During subsequent tests with SO_3 injection, resistivity was found to be in the 10^{10} to 10^{11} ohm-cm range. Figure 1 presents the measured ash resistivity for each condition.

Figure 1: Measured Flyash Resistivity

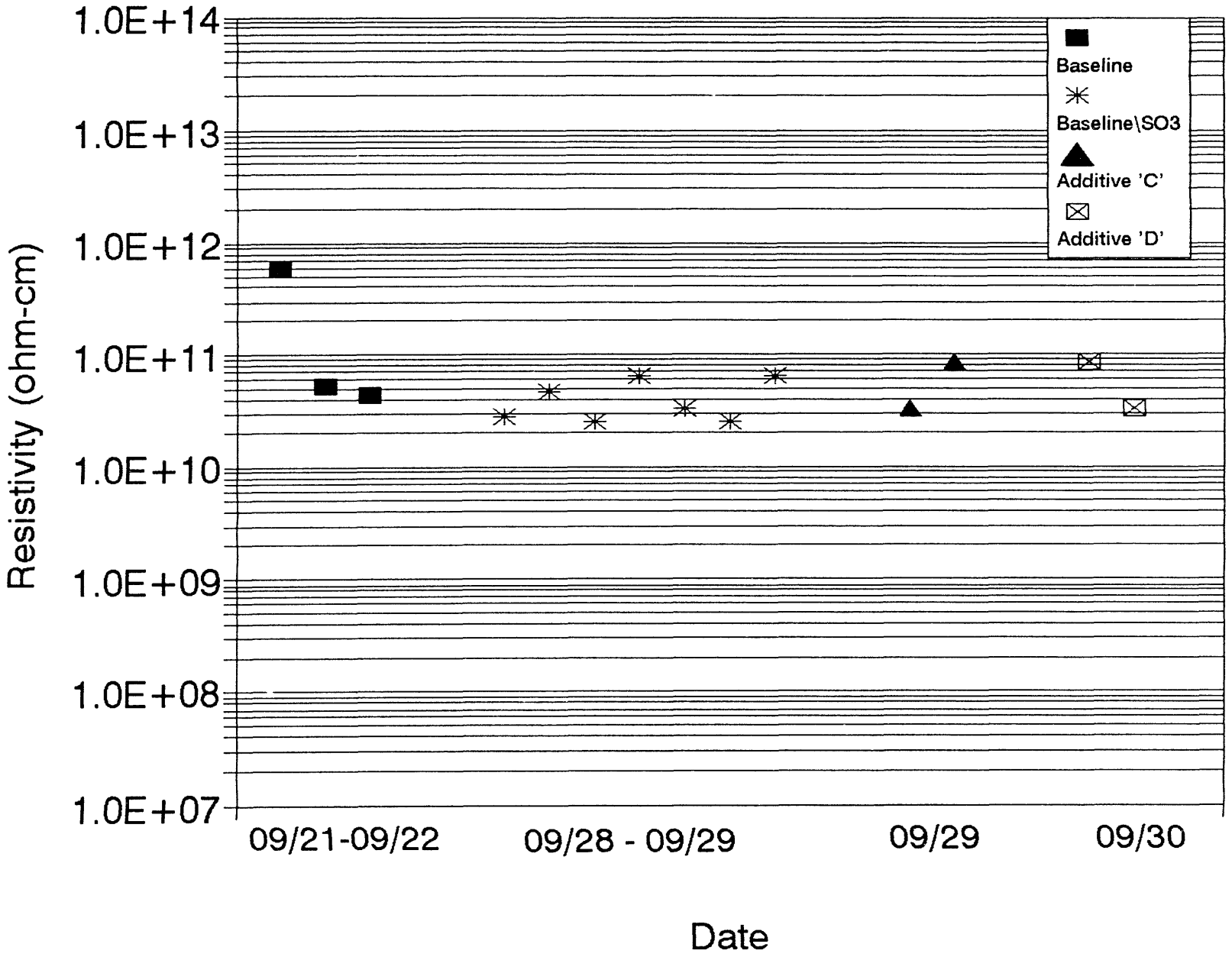

The ADA field resistivity instrument can also measure flue gas acid dew point by a controlled cooling of a view port window, as previously reported (Durham, 1993). During each resistivity measurement, acid deposition on the view port was simultaneously monitored. The observed condensation point was consistently near 180 ^{o}F. This is close to a water dew point and indicates that almost no unreacted SO_3 was present in the flue gas at the ESP inlet. Even at maximum SO_3 conditioning of the system during Week 2, no elevated dew point was detected. This is consistent with the resistivity measurements, which did not show any decrease below 10^{10} ohm-cm during Week 2 of the tests.

Total Particulate

Total particulate concentration was measured simultaneously at inlet and outlet of the ESP, using a heated filter outside the stack in a modified EPA Reference Method 17 train. Inlet and outlet mass tests ran simultaneously for all test conditions. For all tests, a quartz fiber filter media was used instead of standard glass fiber, to avoid potential sample interference due to filter SO_2 uptake in high-SO_2 gas streams.

Stack velocity and flow rate was measured during each run via EPA Reference Method 2. Moisture content was determined for each test using EPA Reference Method 4. Flue gas carbon dioxide content at the ESP inlet and outlet was measured using a portable Fyrite CO_2 analyzer. Oxygen content was periodically measured with a Teledyne fuel cell portable O_2 monitor. Based on measured values of O_2, CO_2, and H_2O, there was minimal air inleakage across the precipitator. It was found, however, that the purge air for the opacity monitor and for the Insitec PCSV-E introduced a significant dilution in the outlet gas stream. This did not affect the mass emission, but it did result in lower measured stack outlet temperatures and mass concentrations.

Table 3 summarizes average particulate test results for each condition during the pilot-scale testing. A more detailed table with data from each test run is also included in Appendix B.

Table 3: Particulate and Opacity Results

Test Condition	ESP Inlet (gr/acf)	ESP Inlet (lb/MBtu)	ESP Outlet (gr/acf)	ESP Outlet (lb/MBtu)	Collection Eff. (%)	Penetration (%)	ESP Outlet Opacity (%
Baseline, 3 fields energized, no SO3	0.408	1.116	0.004	0.012	98.9	1.1	8.3
Baseline with SO3, 2 fields energize	0.393	1.031	0.026	0.073	92.9	7.1	27.2
Additive 'C' with SO3, 2 fields	0.366	0.951	0.030	0.078	91.8	8.2	35.4
Additive 'D' with SO3, 2 fields	0.385	0.996	0.032	0.086	91.3	8.7	34.6

Total particulate loading at the ESP inlet was found to be relatively low by comparison to typical full-size coal combustion processes. Inlet loading ranged from 0.37 - 0.41 gr/acf (0.95 - 1.12 lb/MBtu). Outlet loading was 0.004 gr/ACF (0.012 lb/MBtu) for the baseline condition with 3 fields energized. With two fields energized, the mass loading increased to 0.026 gr/acf (0.073 lb/MBtu). During injection of Additive 'C', outlet loading increased to 0.030 gr/acf (0.078 lb/MBtu). For Additive 'D', the loading again increased, to 0.32 gr/acf (0.086 lb/MBtu).

The increase in mass loading during Week 2 additive injection was accompanied by an increase in outlet opacity over the period. Figure 2 plots the average mass loading at each condition against opacity and against total loading as measured by the Insitec PCSV-E.

Insitec PCSV-E Particle Measurements

A total of 111 Insitec particle size tests were completed over the two week test period. Average total mass measured by the Insitec for each test condition is shown in Figure 2. Total grain loading measured by the Insitec PCSV-E during Week 2 decreased from Week 2 baseline during Additive 'C' injection and then increased for Additive 'D'. The Insitec measurements were consistently higher than mass loading, when plotted on a grains/acf basis. Optical size measured by the Insitec during this test was significantly smaller than the inertial impaction

Figure 2: Opacity vs Outlet Mass

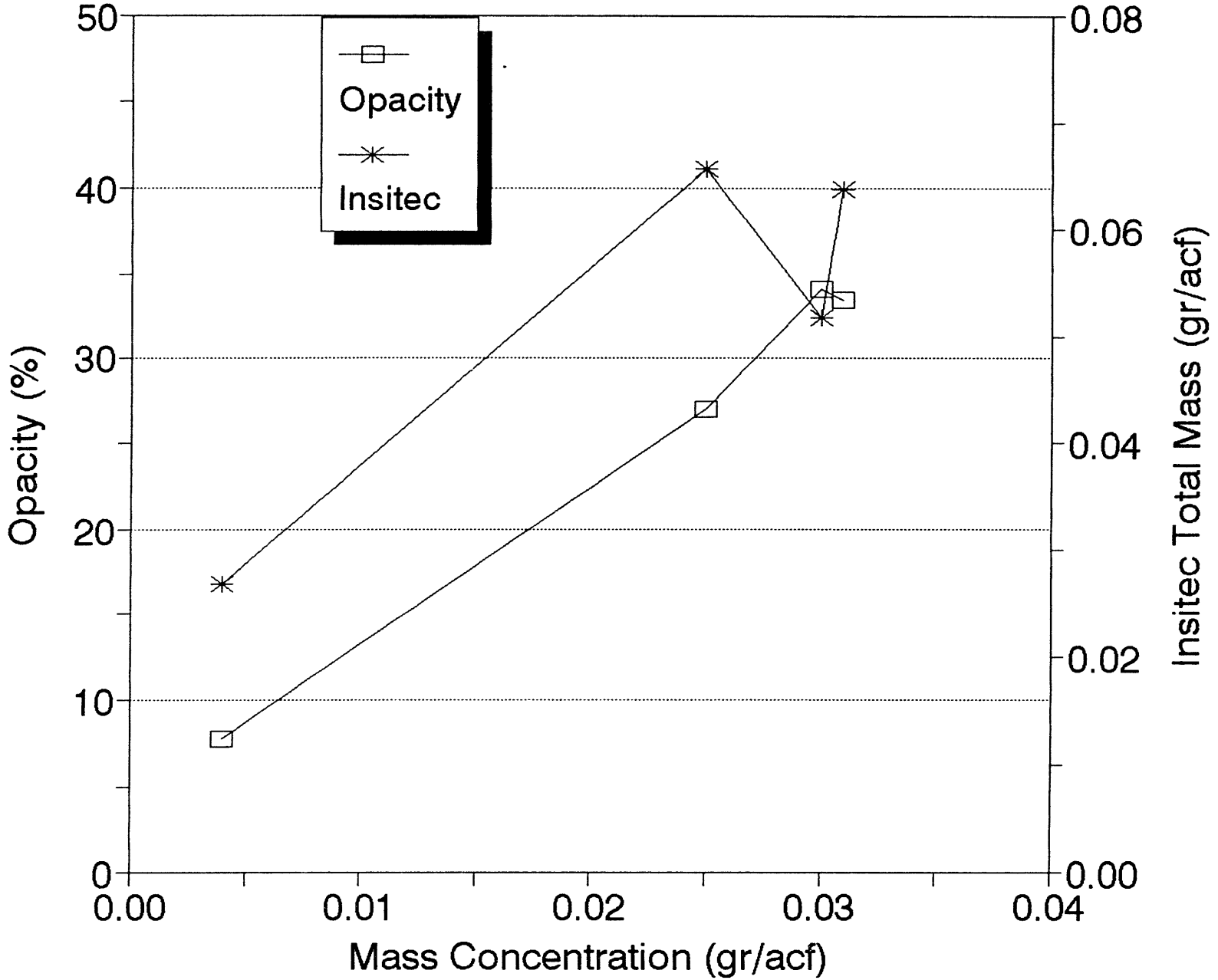

sizing of the cascade impactors. Since the primary objective of the test was to measure relative changes in particle loading, no attempt was made to more closely match reference-method mass loading and particle size with the optical results from the Insitec.

The Insitec responded well to relative changes in mass concentration. This could be clearly seen during two Insitec runs taken during the first week's tests. In the first run, the opacity monitor purge blowers were on and total gas flowrate was approximately 500 acfm at the ESP outlet. In the second run, the blowers were shut off and flowrate decreased to 450 acfm at stack conditions, while conditions in the ESP remained constant. This represents an 11% decrease in flow. The Insitec measured 0.041 gr/acf with the opacity blowers on and 0.035 gr/acf with the blowers off during the same period. This was a decrease of 14% in mass concentration, which agreed well with the flow variation.

Particle Size

Particle size was measured at both the ESP inlet and outlet during Week 1 baseline conditions. Triplicate cascade impactor tests were run at duct center at each location. University of Washington (Pilat) Mark V impactors with right-angle precutters (SoRI/EPA type) were used at the inlet. This impactor has 11 cutpoints, but stages 1 and 2 typically have D_{50} cutpoints above the SoRI/EPA pre-cutter, yielding a 10 stage device with an effective measurement range from about 0.2 to 12 μm. A UW Mark III 7-stage impactor with a right angle nozzle was used at the outlet. Quartz-fiber substrates were utilized for all sample runs. Due to space limitations, the impactors were mounted out of the stack and heated to stack temperature. Inlet and outlet test times were arranged such that an inlet test was completed during each outlet run.

Figures 3 through 6 present the resulting cumulative and differential size distribution, plotted as physical diameter, with a true ash density of 2.5 gm/cm^3. The differential distribution is normalized to the average measured particulate loading from the Method 17 tests at baseline. Normalization corrects a tendency of impactor measurements to understate total mass. Impactor data was reduced using the PCCIDRS Cascade Impactor Data Reduction System, Version 8, as developed by Southern Research Institute (SRI, 1986) from the original cascade impactor data reduction program by the Denver Research Institute (Durham et. al., 1980). Inlet and outlet data is reduced to a set of common particle diameters using a cubic spline fit routine to the raw distribution. Fractional collection efficiency is then calculated at the same diameters for inlet and outlet.

The resulting inlet size distribution had a mass mean diameter (MMD) of 6.3 μm and a geometric standard deviation of 3.5 when fitted to a log-normal distribution. This is relatively small for a coal-fired source, which may be in part due to particle dropout in the combustion chamber. Outlet MMD was 3.0 μm with a geometric standard deviation of 2.5. ESP fractional efficiency at baseline conditions is presented in Figure 7. Maximum penetration of 4.1% occurs in the range 0.5 - 0.8 μm.

Ash Analysis and Predicted Resistivity

Elemental analysis of a blended hopper ash sample taken during the test is given in Table 4. Using this ash composition, fly-ash resistivity was predicted using the Bickelhaupt empirical computer model. In the model, predictions are made for resistivity at various concentrations of SO_3. For this analysis, the SO_3 was assumed to be 1 ppm or less, as was measured at the ESP inlet. The model predicted a resistivity of 4.4×10^{10} ohm-cm at stack temperature with 1 ppm SO_3. This is somewhat lower than the measured resistivity and does not conclusively demonstrate high resistivity conditions. However, it is higher than would be expected for an Eastern bituminous coal.

Table 4. Elemental Analysis of Hopper Flyash

Constituent	Percent by Weight
SIO_2	44.98
AL_2O_3	24.18
TIO_2	1.10
FE_2O_3	13.88
CAO	5.18
MGO	0.79
NA_2O	0.94
K_2O	1.47
P_2O_5	0.69
SO_3	5.93
Total	99.14

Figure 3: Cumulative Size Distribution
ESP Inlet: Baseline

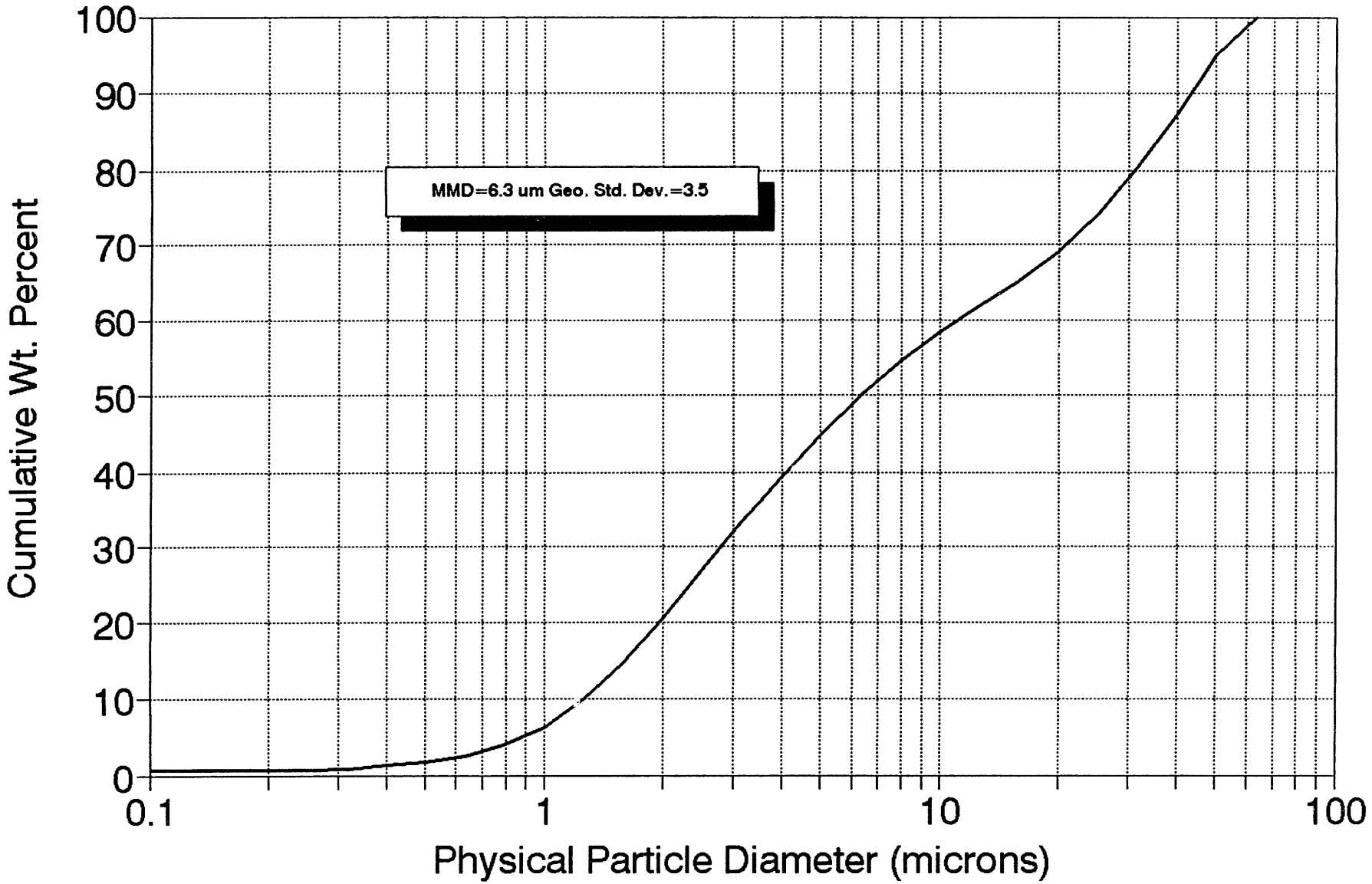

Figure 4:Differential Size Distribution
ESP Inlet: Baseline

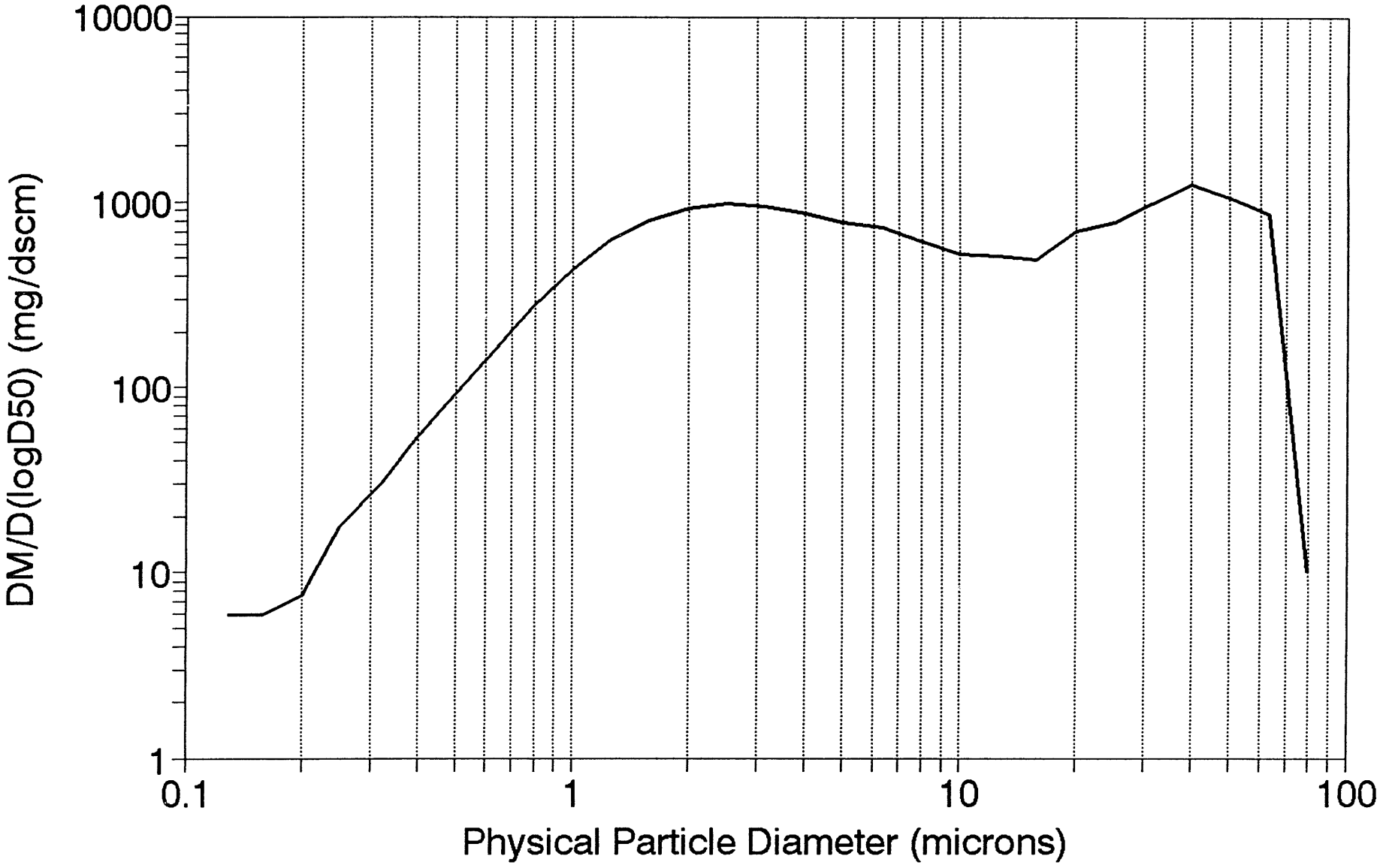

Figure 5: Cumulative Size Distribution
ESP Outlet: Baseline

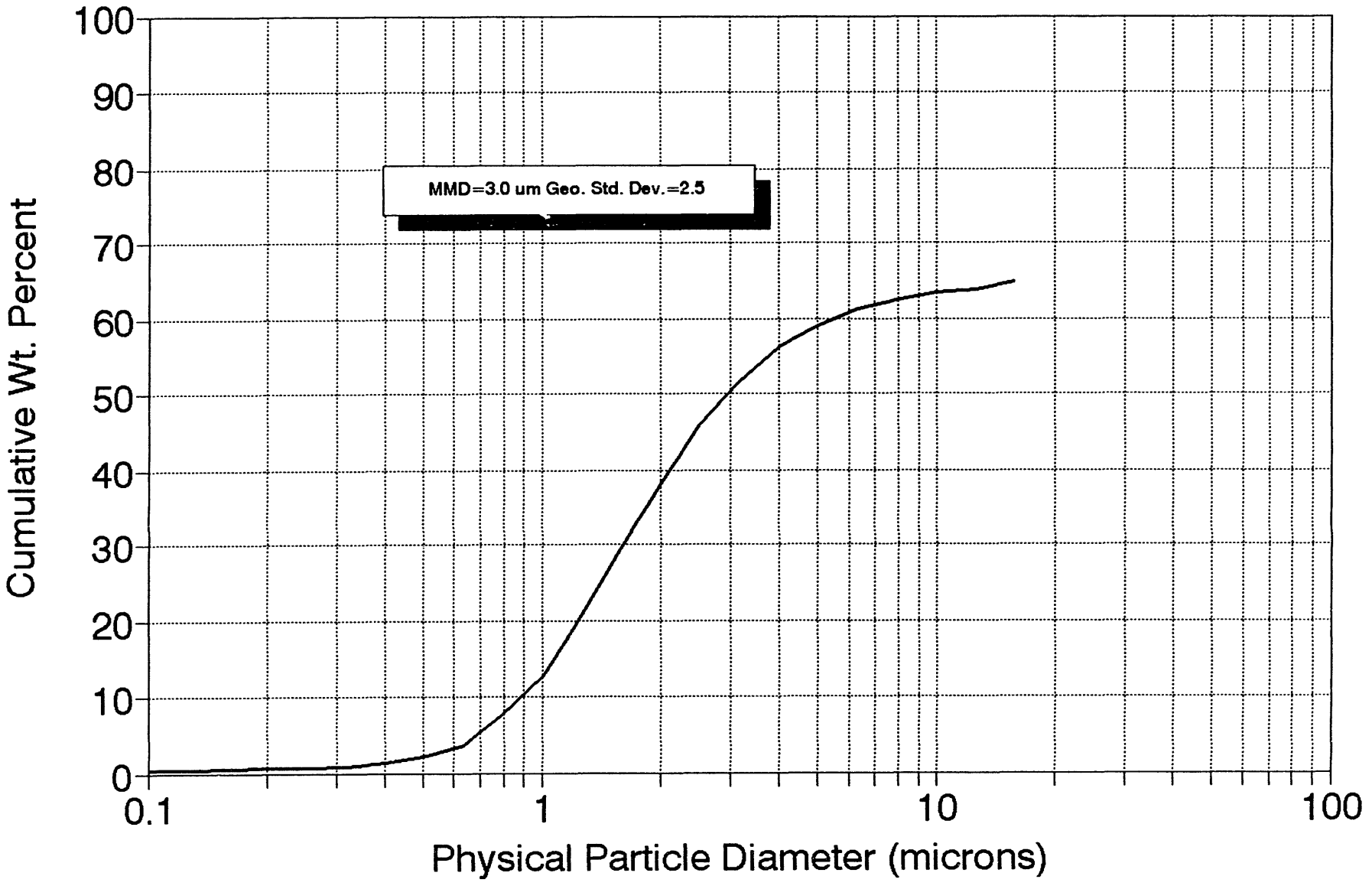

Figure 6:Differential Size Distribution
ESP Outlet: Baseline

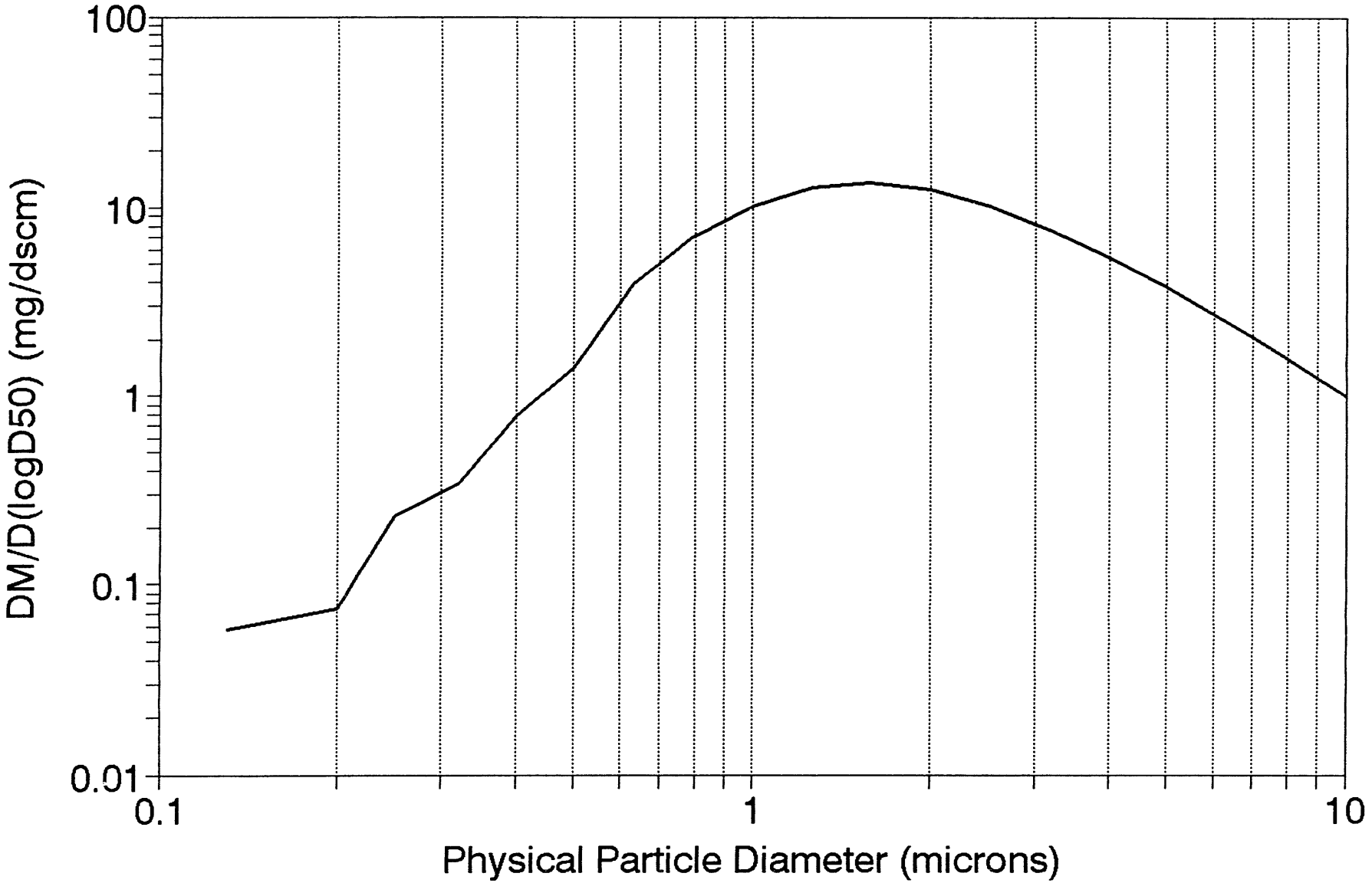

Figure 7: ESP Fractional Penetration
Baseline (3 Fields)

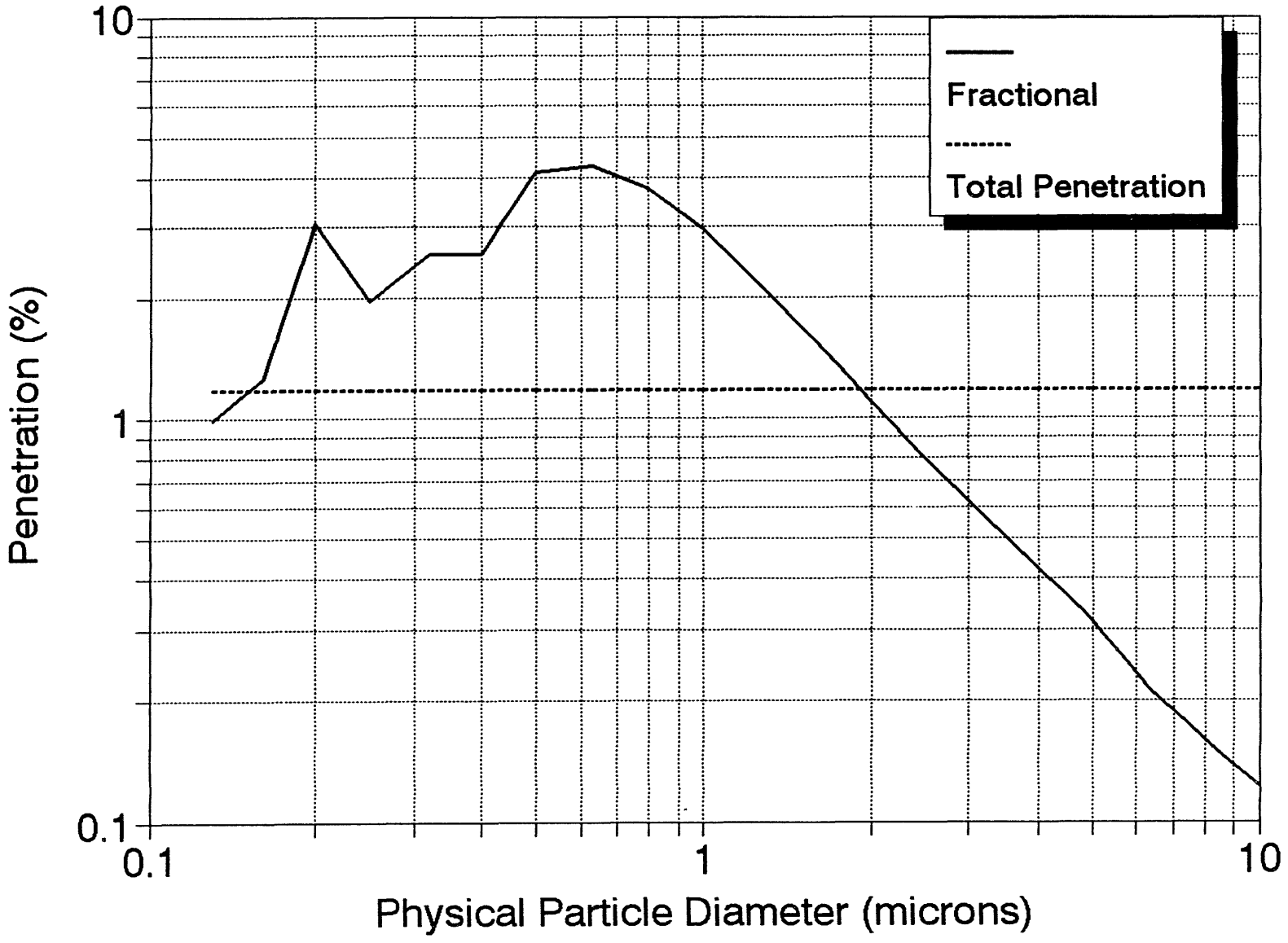

ESP Modeling of Observed Mass and Opacity Variations

It was hypothesized that the observed changes in outlet mass loading and opacity during Week 2, from baseline to Additive 'C' and Additive 'D' injection, could be entirely due to additive solids exiting the ESP unreacted as sub-micron particulate. If this were the case, the additives would have no effect on ESP performance, but could be contributing to increased outlet mass loading and opacity.

The measured increase in outlet mass from Week 2 baseline to additive injection was 0.019 lbs/hr for Additive 'C' and 0.026 lbs/hr for Additive 'D' (see Appendix B). It was calculated that the total mass of additive solids was 0.003 lbs/hr at the test injection rate. Based on this, the additive solids could have contributed at most 16% of the observed increase for Additive 'C'. Therefore, the introduction of additive solids alone could not explain the observed mass difference.

The analysis for opacity is more complex, since opacity depends not only on particulate amount, but on particle size and refractive index. Outlet opacity increased from an average of 27.2% at baseline to 35.4% during Additive 'C' testing. To analyze the measured opacity difference, the CONSOL ESP was modeled using the ADA ESP model, at the operating conditions measured during the pilot-scale tests.

The ADA ESP model has a subroutine to predict the opacity due to the scattering and absorption of the particles penetrating the ESP. The opacity is a function of particle size, concentration, and composition, and the optical path length. For particles greater than 1 μm, the light extinction is determined by the total projected area of the aerosol particles. However, for smaller particles, the composition of the particle plays an important role, and the theory developed by Mie (1908) is used to calculate the opacity. These relationships, which are described in detail by Ensor (1972), can be used to calculate the extinction coefficient of particles as a function of the refractive index of the particle and the diameter of the particle relative to the wavelength of light. In order to calculate the opacity, the ESP model predicts the number of particles in each size interval, calculates the extinction coefficient for each interval, and then determines the sum of all size ranges.

For this application, a worst-case condition was modeled to determine the possible impact of additive injection on ESP outlet opacity. In this scenario, it was assumed that all of the particles resulting from evaporation of additive spray droplets would enter the ESP as a sub-micron aerosol, with no interaction with entrained flyash or with the duct surfaces. It was

calculated that particle size resulting from evaporation of the additive spray droplets would be approximately 0.7 μm, assuming a particle density of 2.0 gm/cm^3 and spherical particles. Particles in this size range exhibit strong scattering of light in the 0.4 - 0.7 μm wavelength range which opacity monitors respond to.

In the ADA ESP model, there are several "non-ideal" parameters which must be customized to the particular ESP. These include a velocity distribution parameter, gas sneakage fraction, and non-rap reentrainment fraction. For the CONSOL ESP, the model was first run at initial baseline conditions, to determine the correct values for the gas sneakage and non-uniform velocity distribution factors. Once established, these parameters would not change for any of the later test conditions.

At baseline, the non-rapping reentrainment fraction was initially set to 0.01, which corresponds to minimal non-rapping reentrainment. This factor was applied for two reasons. First, the outlet opacity during the Week 1 baseline exhibited almost no spikes which were not related to rapping (Figures A.1 and A.2, Appendix A). In addition, the particle resistivity is in a range which is expected to minimize reentrainment.

A total of 4 ESP model runs were completed to characterize the ESP outlet opacity, as summarized in Table 5. In all of the model runs, particle refractive index was assumed to be that for an eastern bituminous coal fly-ash, 1.5 - 0.0043i (Cowen and Ensor, 1982). For materials other than strong light absorbers such as carbon, this will be a good approximation.

Using 0.01 for non-rapping reentrainment, the model predicted outlet opacity to be 10.3%, compared to a measured value of 8.3%. Predicted opacity was higher than measured for this condition. However, the model could not compensate for dilution in the outlet duct from the opacity monitor and the Insitec PCSV-E instrument air purge. Given a total system flow of only 500 cfm, the purge air created a significant dilution of stack gas, which would have reduced measured opacity. Predicted particulate penetration was 1.4%, while measured penetration was 1.1%. The fact that actual penetration was in good agreement to the model prediction values indicates that non-rapping reentrainment was minimal for this condition.

The model was next run to match ESP performance at baseline conditions with two fields and SO_3 injection, using 0.10 for the gas sneakage and the velocity distribution parameters. The effect of SO_3 conditioning was incorporated indirectly into the model through input of the measured ESP electrical characteristics.

Table 5. ESP Modeling Summary

Model Condition	Purpose	Opacity	Mass Penetration
Baseline conditions with 3 electrical fields	Establish gas sneakage and velocity factors. Best value is 0.10 for sneakage and velocity factors with non-rap reentrainment of 0.01.	Predicted is 10.1%, measured is 8.3%.	Predicted mass penetration is 1.4%, measured is 1.1%.
Baseline with SO3 conditioning and 2 field ESP.	Establish non-rap re-entrainment for 2 field operation. Optimal non-rap reentrainment value is 0.20	Predicted is 34.5%, measured is 27.2%. Purge air dilution after ESP reduces actual opacity.	Predicted mass penetration is 6.3%, measured is 7.1%.
Additive injection, adjusted inlet particle size.	Determine the maximum effect of Additive 'C' on outlet opacity if all additive enters ESP as sub-micron spheres.	Predicted opacity is 34.8%, less than 1% change from previous.	Predicted mass penetration is 6.4%, nearly identical to previous.
Baseline/SO3 with increased mass loading to simulate Additive 'C' outlet loading.	Determine what effect the change in mass loading from baseline to Additive 'C' has on opacity.	Predicted opacity is 40.4%, measured is 35.4%.	Model run set to match particulate penetration during Additive 'C' test.

This run established an optimal value of 0.20 for non-rapping reentrainment during 2 field operation of the ESP. Predicted opacity for this run was 34.5%, while measured opacity was 27.2%. Again, the model is expected to overpredict opacity because purge air dilution cannot be simulated. Predicted mass penetration was 6.3% for this condition, which agreed well with a measured value of 7.2%.

The model was then with an adjusted inlet particle size distribution to simulate the worst-case effect of additive injection on opacity. A total of 4.3 x 10^{12} particles/hr would be generated for a particle size of 0.7 μm with a density of 2.0 gm/cm^3. To simulate this in the ESP model, the added particles were inserted into the measured inlet mass size distribution at 0.7 μm, taking into account the change in density between additive solids and particle flyash (2.5 gm/cm^3).

With this adjusted particle size, the model predicted an outlet opacity of 35.3%. This was less than a 1% change from the predicted value at Week 2 baseline and much less than the measured opacity change of 8.3% from Week 2 baseline to Additive 'C'. The predicted mass penetration for this run was 6.4%, only slightly higher than predicted for Week 2 baseline (6.3%). This clearly indicates that the effect of additive injection on outlet opacity and mass loading, when considered by itself, would not account for the observed differences.

A final model run was completed to determine the effect of the measured increase in outlet mass loading during the Additive 'C' test on predicted outlet opacity. The model was run as for Week 2 baseline, except that particulate loading was increased to match the Additive 'C' outlet mass emission of 0.137 lbs/hr. Predicted opacity for this run increased from the Week 2 baseline of 34.5% to 40.4%. When the effects of outlet dilution are considered, this agreed well with the measured increase from 27.2% to 35.4%.

From this final model run, we conclude that the observed opacity changes from Week 2 baseline to additive injection are consistent with what would be expected given the measured increase in outlet mass.

Conclusions

The pilot-scale tests indicate that ESP performance decreased during the additive injection period. However, it is unclear if the performance decrease was due to the effect of the additives or to an unrelated shift in ESP baseline operation. The opacity decreased somewhat during the final baseline condition, but the ESP did not fully recover to the initial Week 2 baseline.

ESP operating conditions during the initial pilot-scale tests were not well-matched to the target conditions where increased particle adhesion could have a beneficial effect on ESP performance. High resistivity meant that reentrainment was already minimal and little, if any, improvement would be expected. If the additives were further increasing particle cohesion and contributing to plate surface buildup, in a high resistivity situation, the ash layer would be even harder to remove, potentially decreasing performance. Thus, it is possible that the additives were performing as anticipated, but were simply not in the correct operating regime. Examination of Fields 2 and 3 load cell data during Week 2 of testing, as shown on Figures A.5 through A.8, shows steadily increasing ash layer buildup which periodic rapping did not remove.

The only conclusive way to determine additive effectiveness will be to test under conditions where non-rapping reentrainment seriously decreases ESP performance, in the range of 10^7 to 10^9 ohm-cm ash resistivity. The electrostatic forces are relatively flat in this range, as shown in Figure 8, so that changes in flue gas conditions that will result in a change in resistivity by up to two orders of magnitude will have little effect on the magnitude of reentrainment. Also, at the very low resistivity conditions, reentrainment will be the highest and performance improvements will be easier to measure.

The effect of particle resistivity on ESP collection efficiency is closely related to the dust electrostatic holding force. Figure 9 illustrates this relationship based on previous ADA work with TVA at Shawnee Power Station on a spray dryer/ESP. It is seen that the collection efficiency for a well-performing ESP changes rapidly for resistivity between 10^9 to 10^{10} cm. This is exactly the region in which electrostatic holding forces are increasing most rapidly, as shown in Figure 8.

Finally, the ESP modeling analysis of opacity demonstrates that the injection of any of the additives in the concentrations envisioned in this program will have, at most, a small effect on outlet opacity, which is an important result independent of the pilot-scale tests.

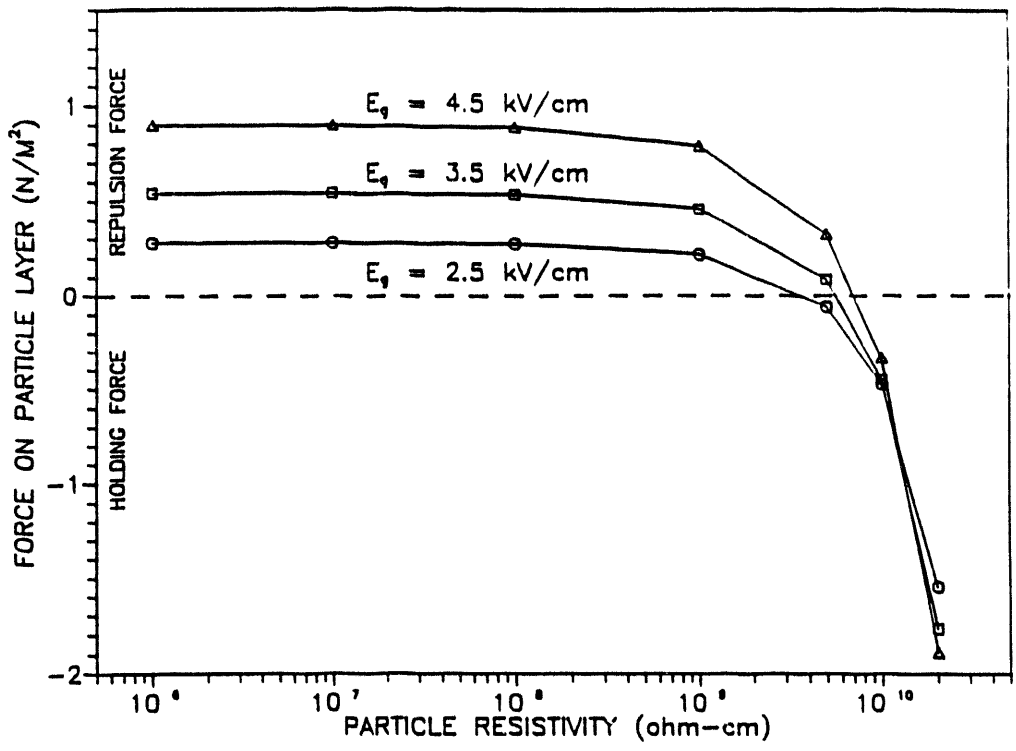

Figure 8. Electrostatic Forces On A Dust Layer In An ESP

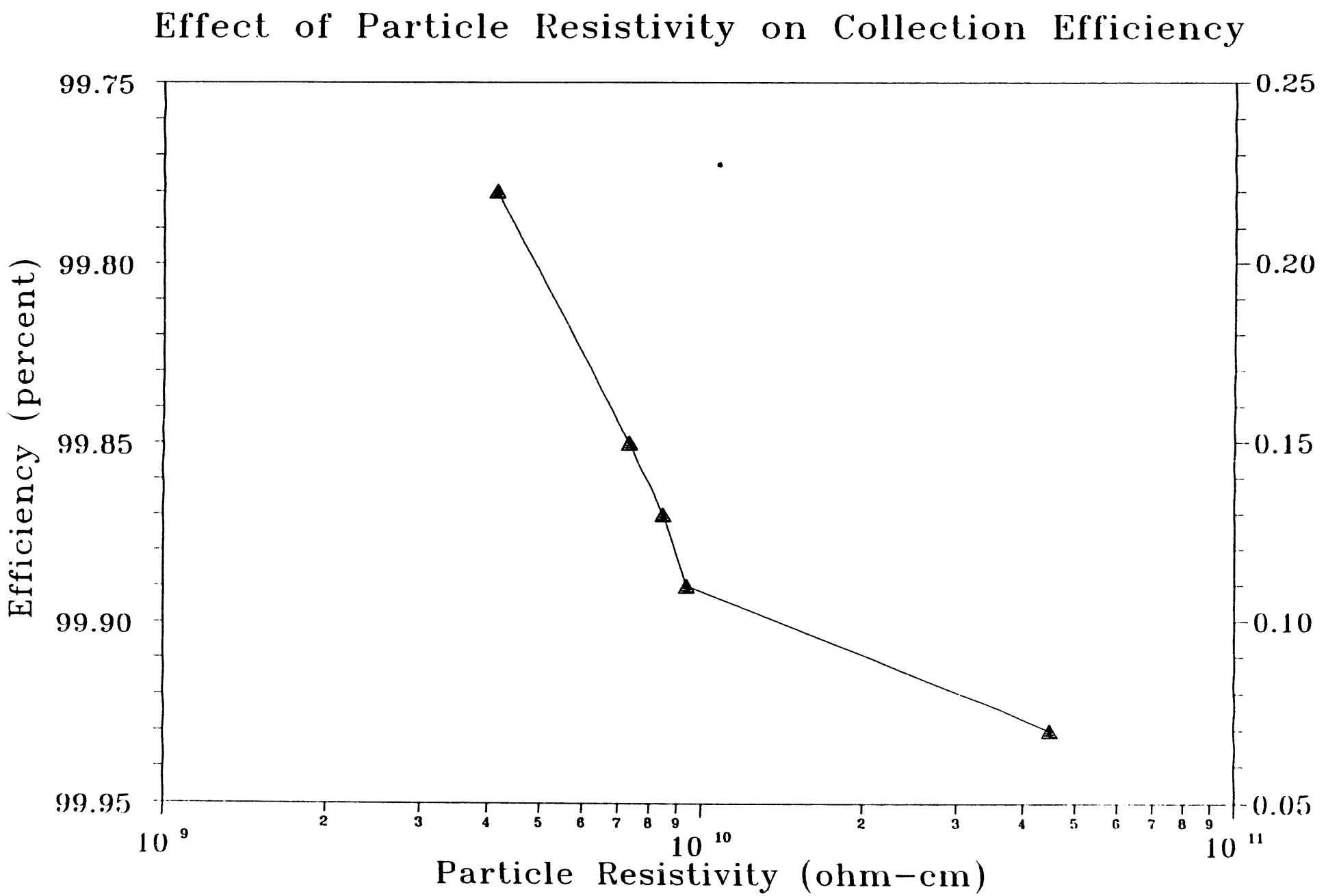
Effect of Particle Resistivity on Collection Efficiency
Efficiency (percent)
99.75
99.80
99.85
99.90
99.95
0.25
0.20
0.15
0.10
0.05
10 9
2
3
4
5
6
7
8
9
10 10
2
3
4
5
6
7
8
9
10 11
Particle Resistivity (ohm-cm)

Figure 9

References

Durham, M.D., "Flue Gas Conditioning for Inproved Particle Collection in Electrostatic Precipitators", First Topical Report, ADA Report No. 4300-93-T1, prepared for the U.S. Department of Energy, April, 1993.

Southern Research Institute, Procedures Manual For The Recommended ARB Particle Size Distribution Method, prepared for the California Air Resources Board, 1986.

Durham, M.D. et. al., Cascade Impactor Data Reduction System For TRS-80, Denver Research Institute and EPA IERL, 1980.

Cowen, S. J. and Ensor, D. S. "The Relationship of Fly Ash Light Absorption to Smoke Plume Opacity," Proceedings: EPA Third Symposium on the Transfer and Utilization of Particulate Control Technology, Volume 4, EPA-600/9-82-005d, 1982 p. 271.

Ensor, D.S. "Smoke Plume Opacity Related to the Properties of Air Pollutant Aerosols," Ph.D. Dissertation, University of Washington, 1972.

Mie, G. "Beitrage zur Optik truber Medien, Speziell Kolloidaler Metallosunge," Ann. Physik. 25:377-455, 1908.

Appendix A

ESP Operating Conditions During Pilot-Scale Tests

Figures A.1 through A.4: Week 1 Testing

Figures A.5 through A.8: Week 2 Testing

Outlet Opacity

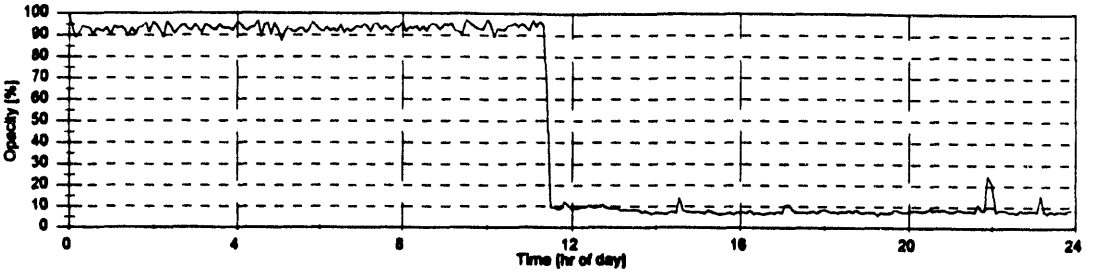

Field 1 Voltage & Current

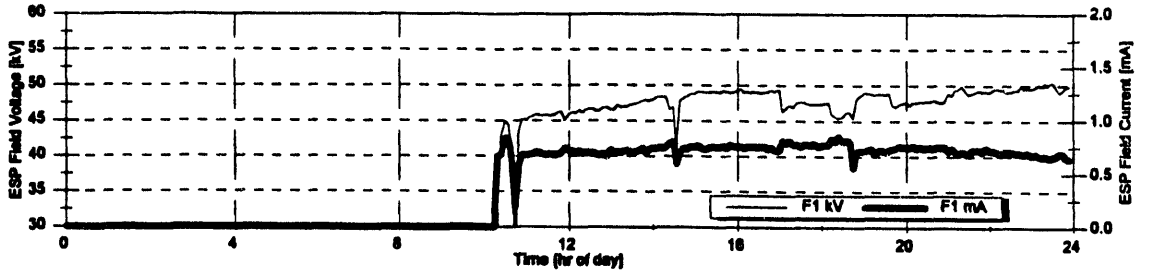

Field 2 Voltage & Current

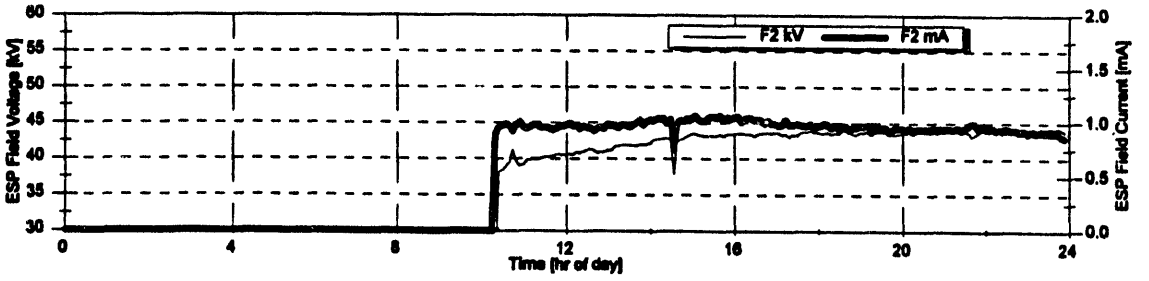

Field 3 Voltage & Current

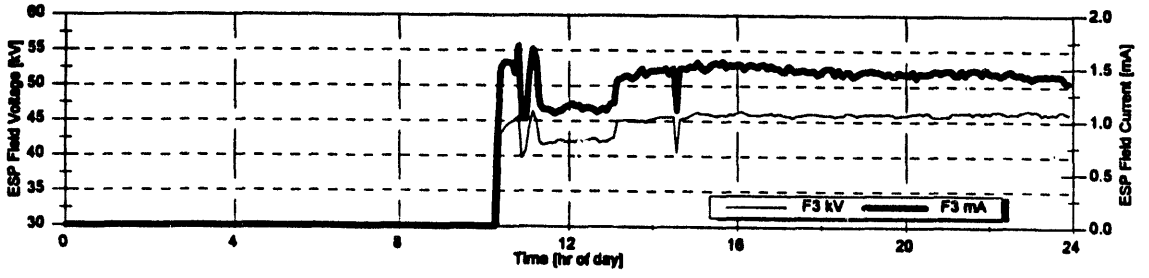

Plate Mass

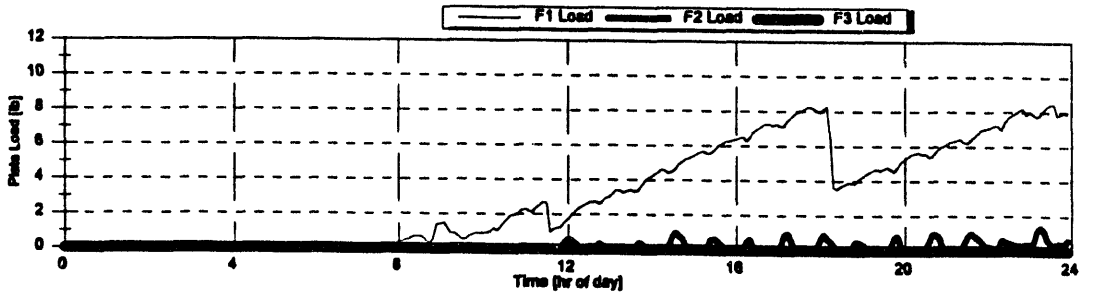

Test Conditions

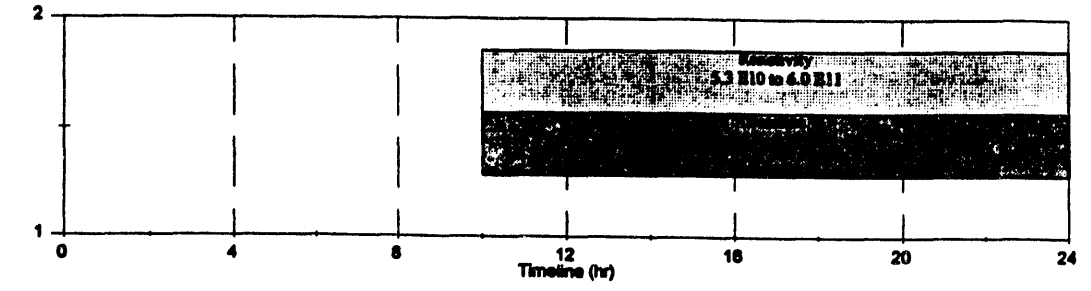

Figure A.1: 09/21/93 ESP Data

Outlet Opacity

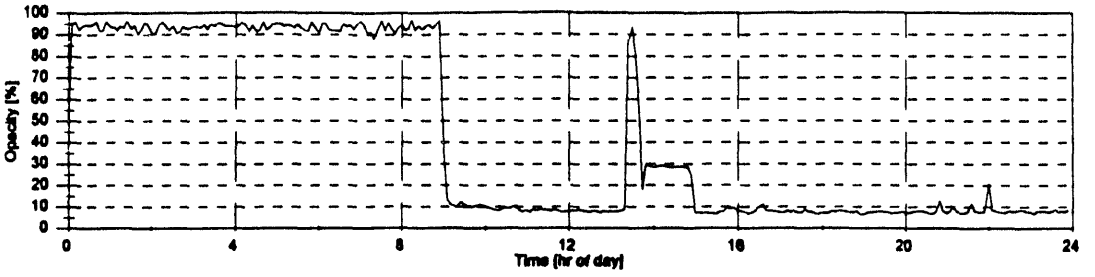

Field 1 Voltage & Current

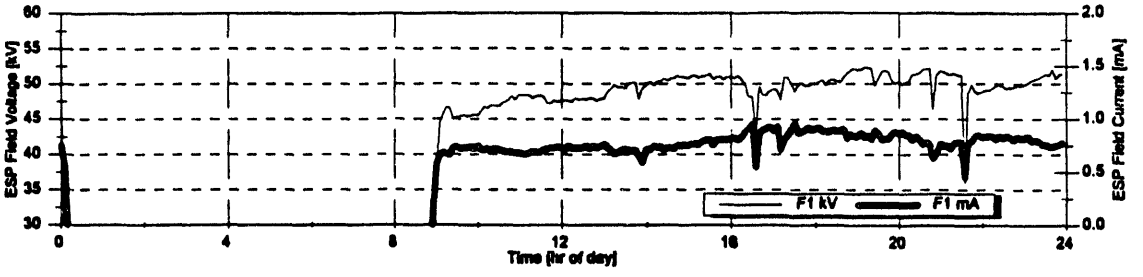

Field 2 Voltage & Current

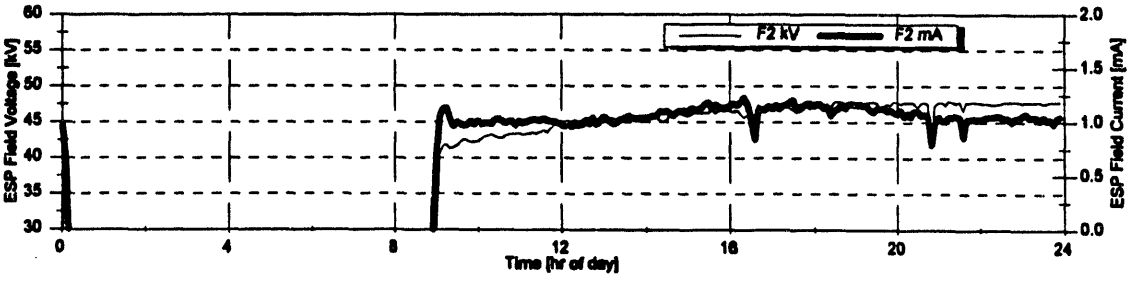

Field 3 Voltage & Current

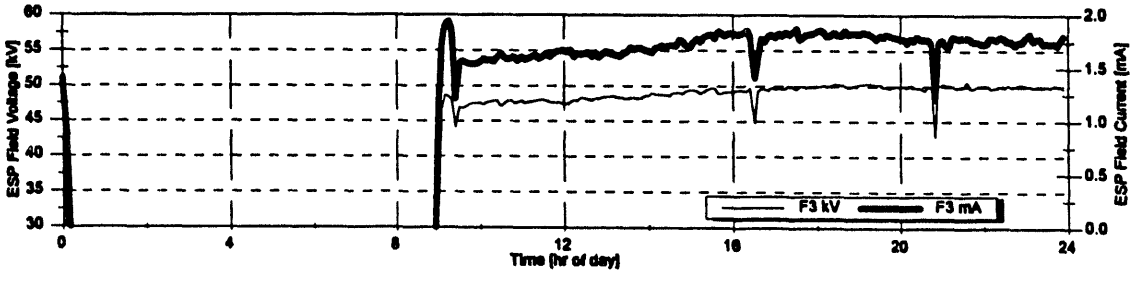

Plate Mass

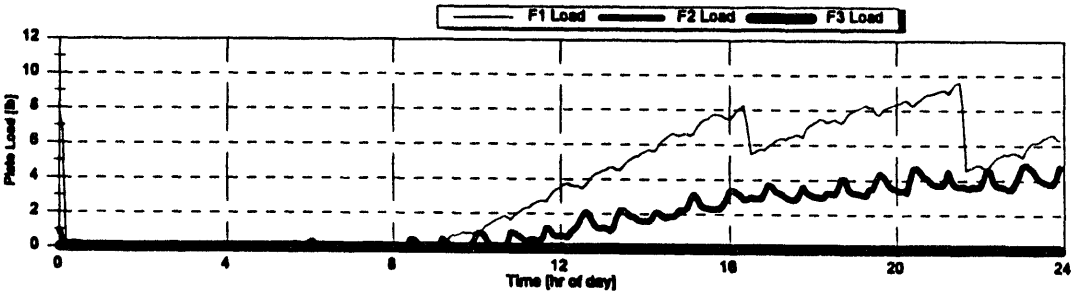

Test Conditions

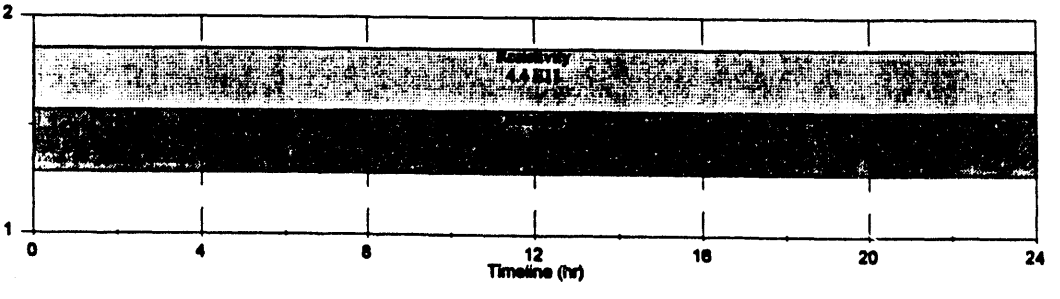

Figure A.2: 09/22/93 ESP Data

Outlet Opacity

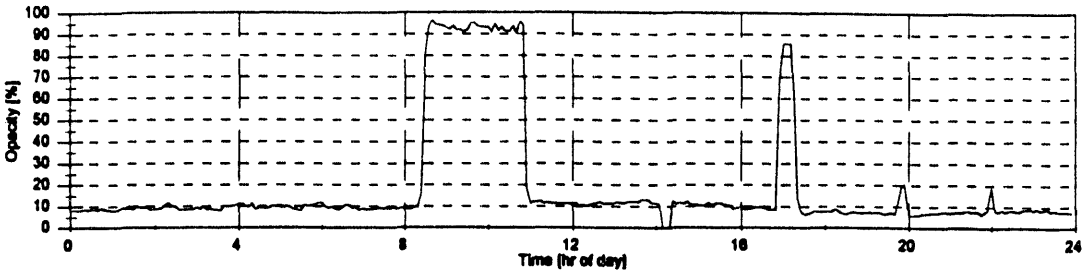

Field 1 Voltage & Current

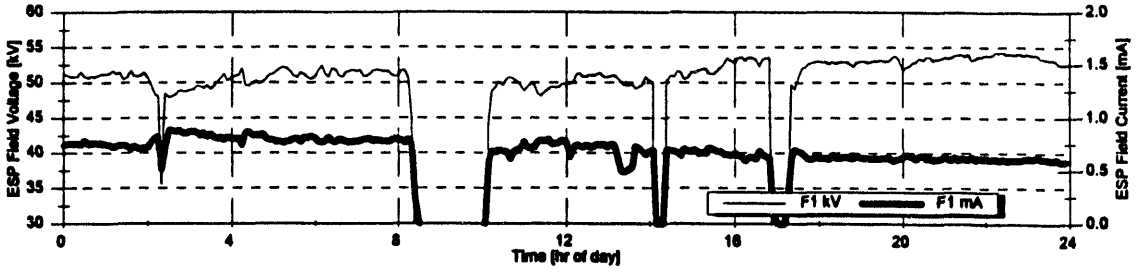

Field 2 Voltage & Current

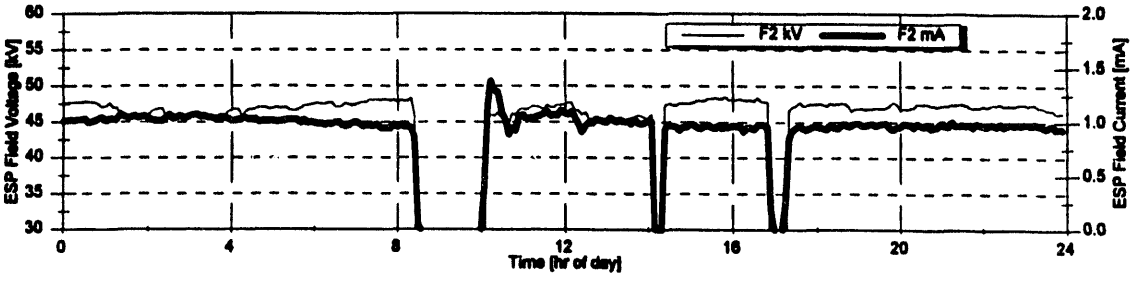

Field 3 Voltage & Current

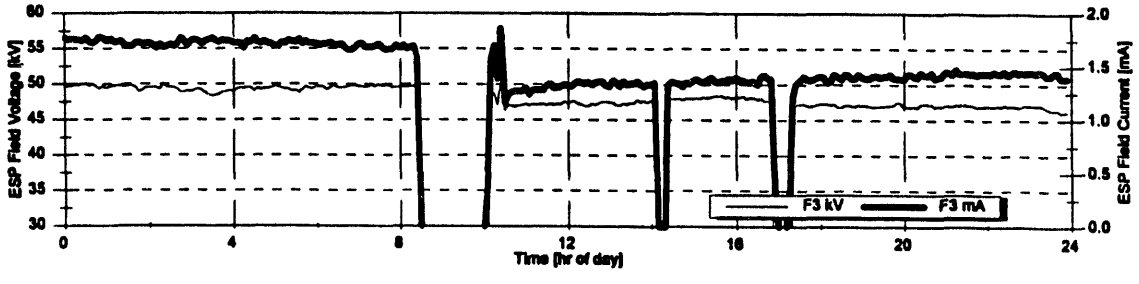

Plate Mass

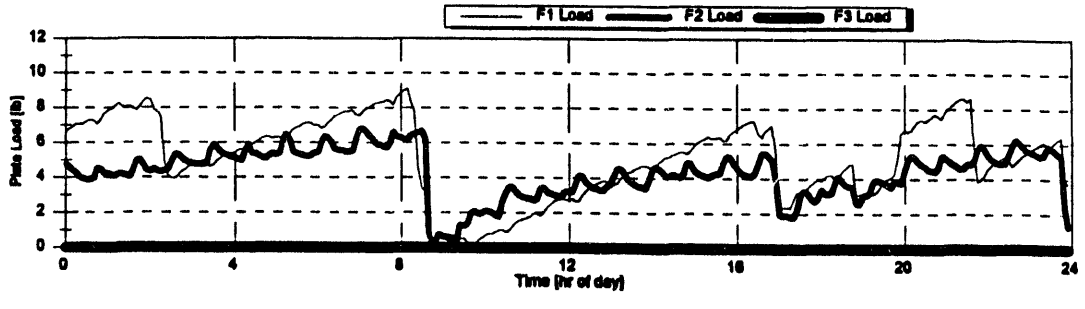

Test Conditions

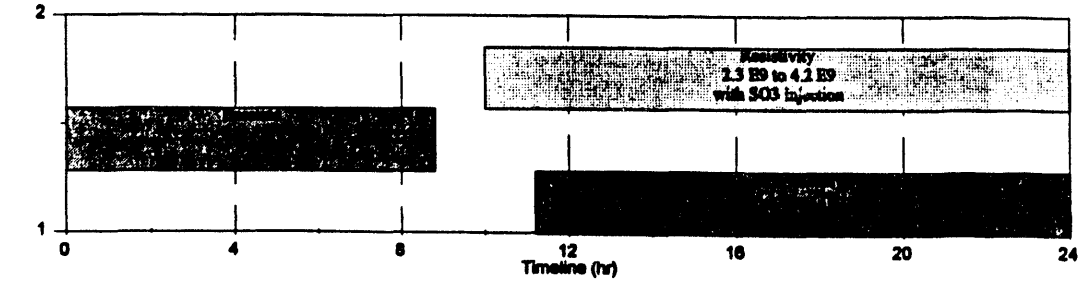

Figure A.3: 09/23/93 ESP Data

Outlet Opacity

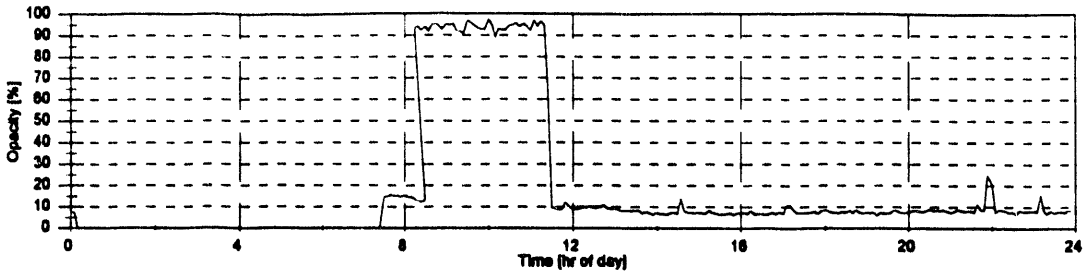

Field 1 Voltage & Current

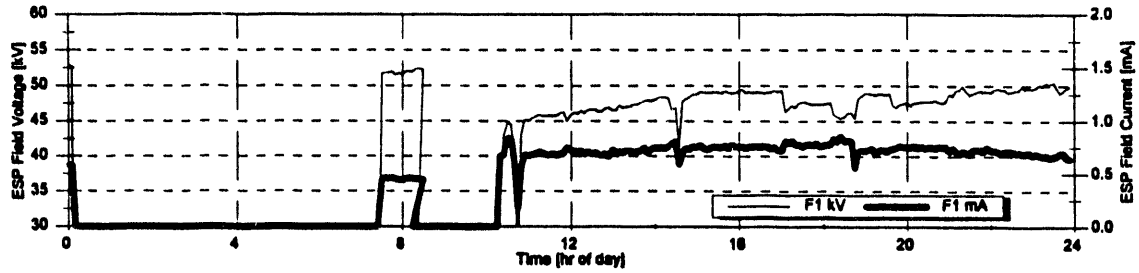

Field 2 Voltage & Current

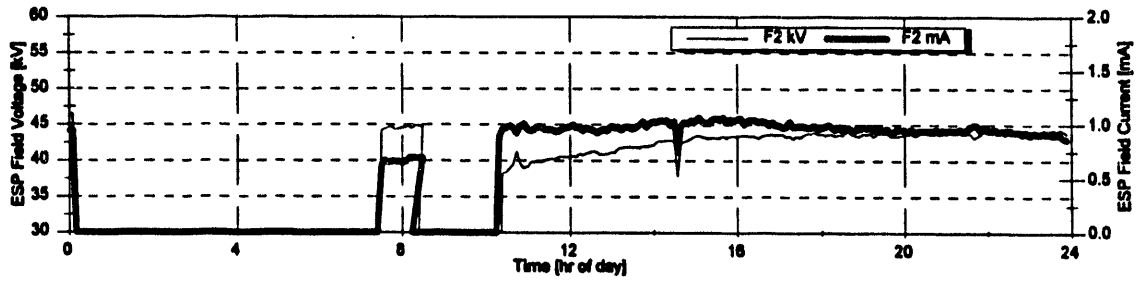

Field 3 Voltage & Current

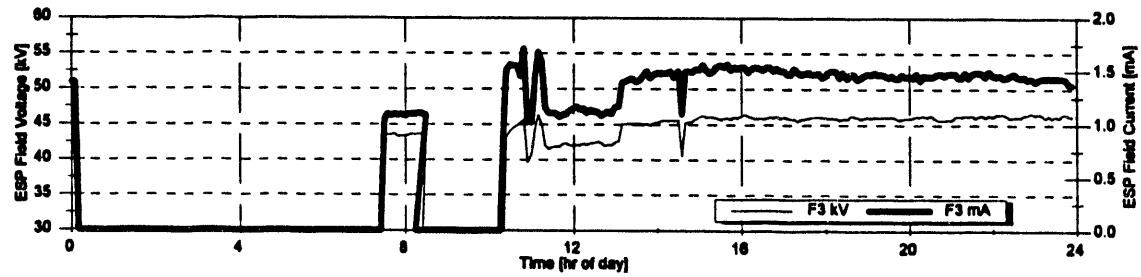

Plate Mass

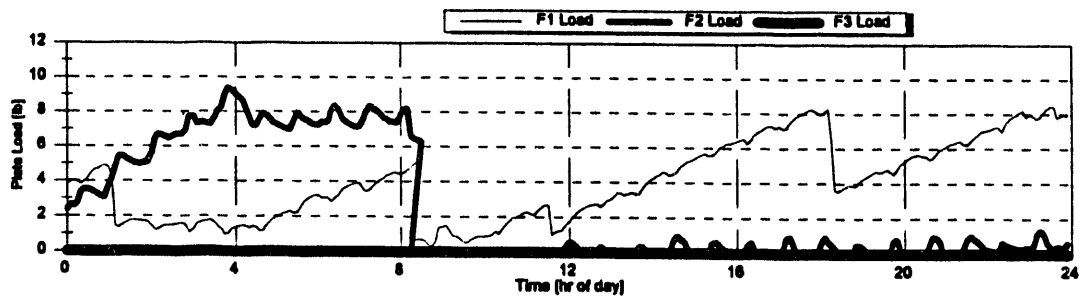

Test Conditions

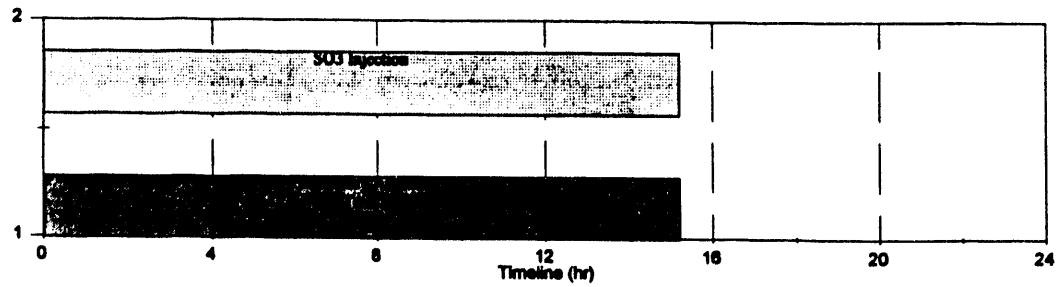

Figure A.4: 09/24/93 ESP Data

Outlet Opacity

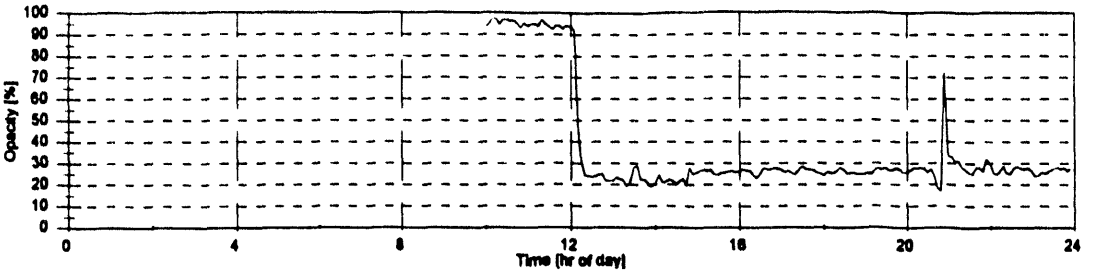

Field 1 Voltage & Current

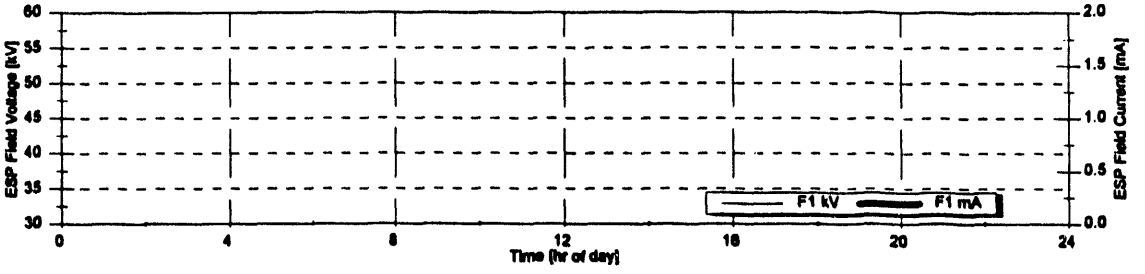

Field 2 Voltage & Current

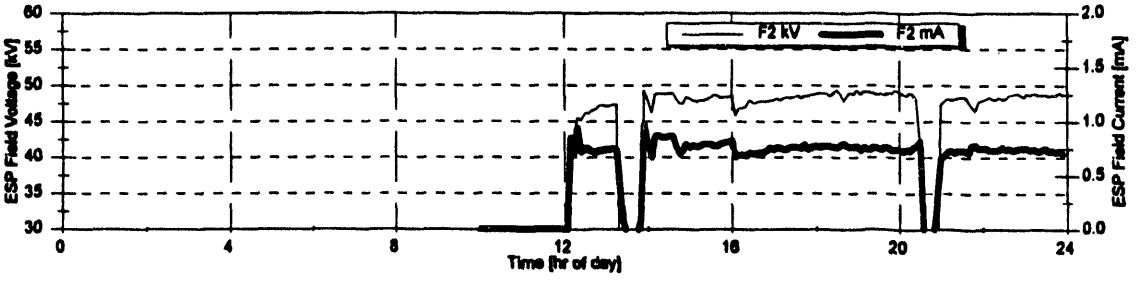

Field 3 Voltage & Current

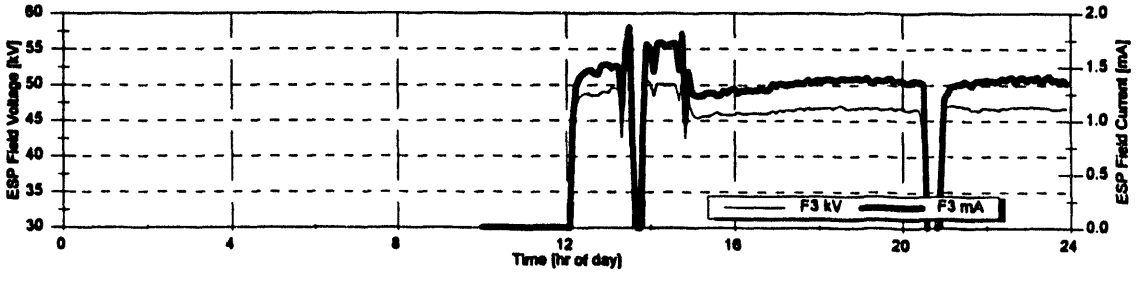

Plate Mass

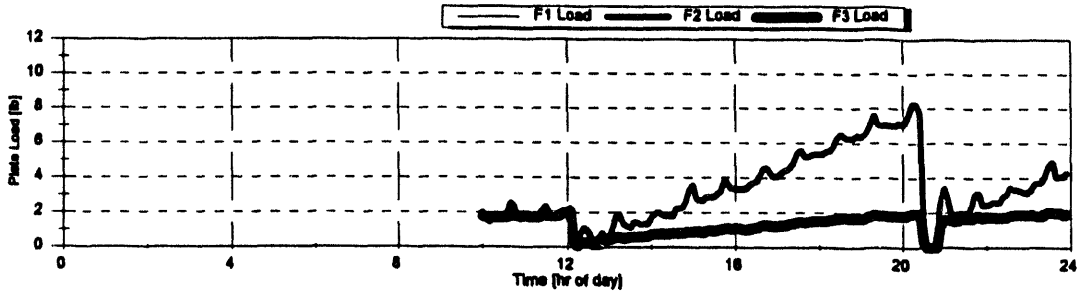

Test Conditions

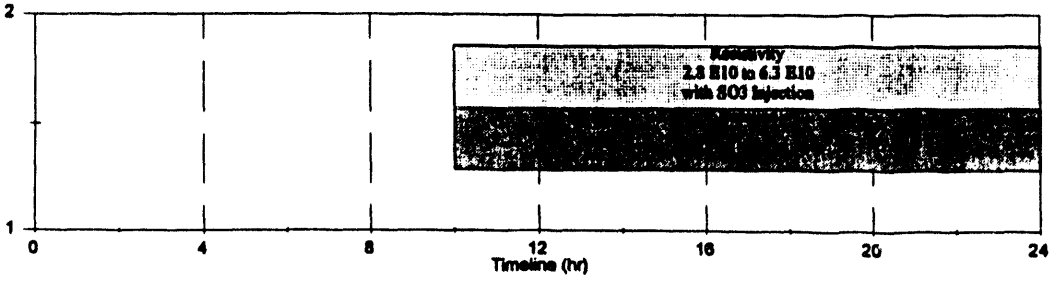

Figure A.5: 09/28/93 ESP Data

Outlet Opacity

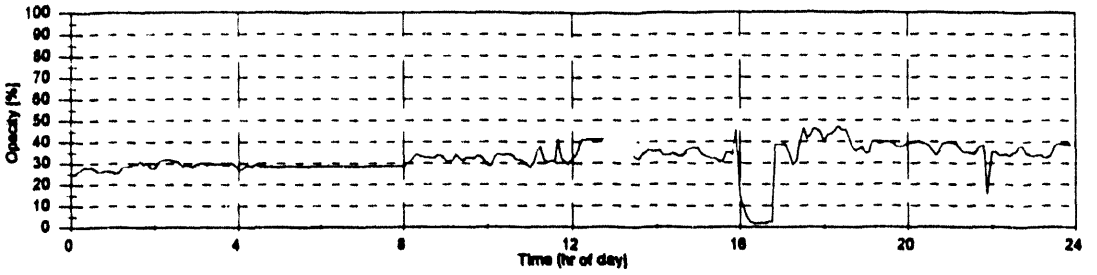

Field 1 Voltage & Current

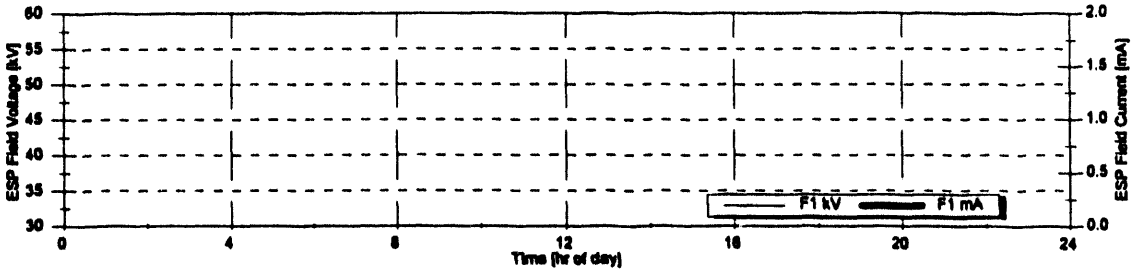

Field 2 Voltage & Current

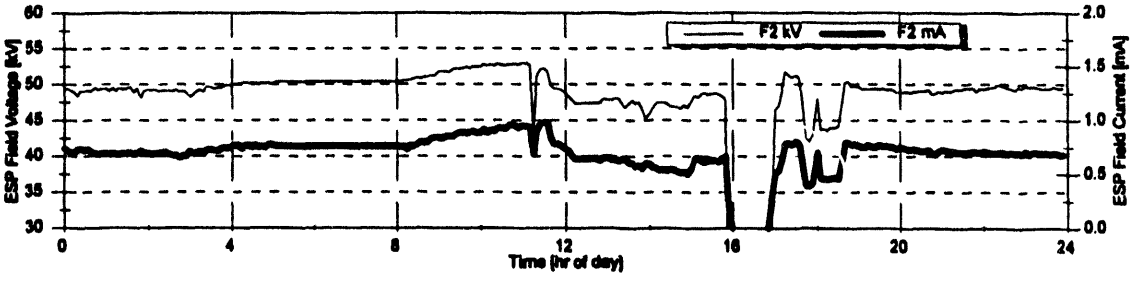

Field 3 Voltage & Current

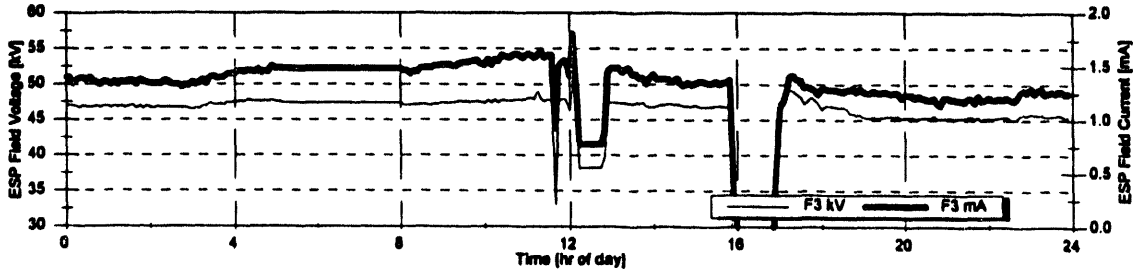

Plate Mass

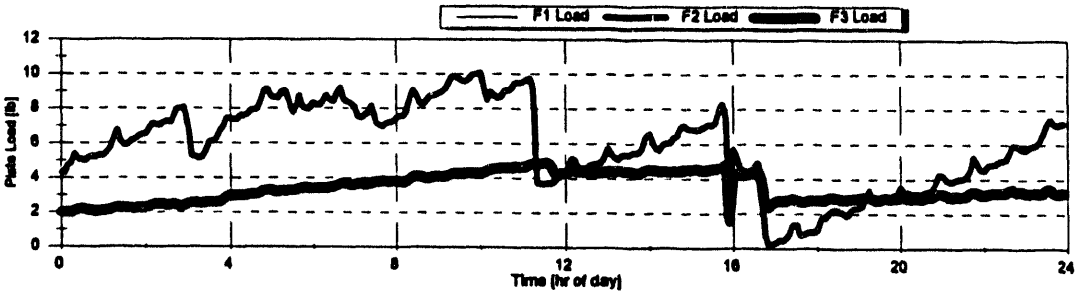

Test Conditions

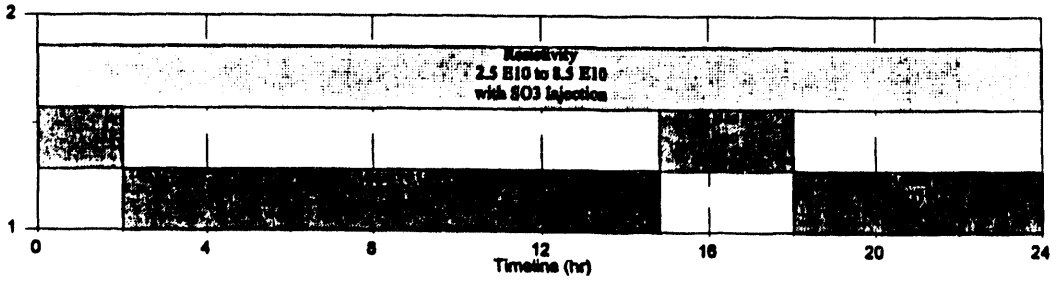

Figure A.6: 09/29/93 ESP Data

Outlet Opacity

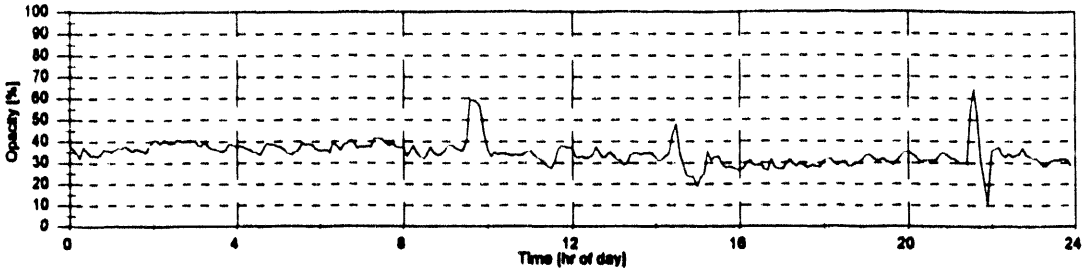

Field 1 Voltage & Current

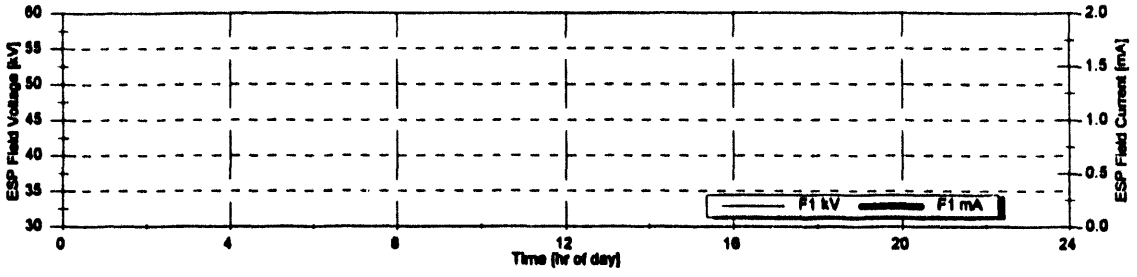

Field 2 Voltage & Current

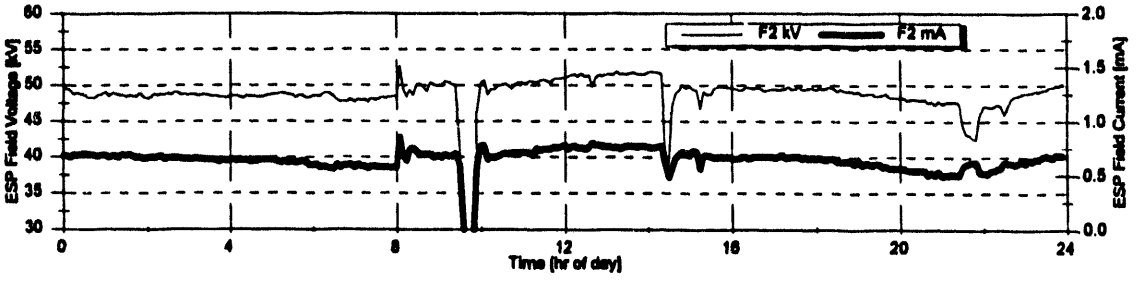

Field 3 Voltage & Current

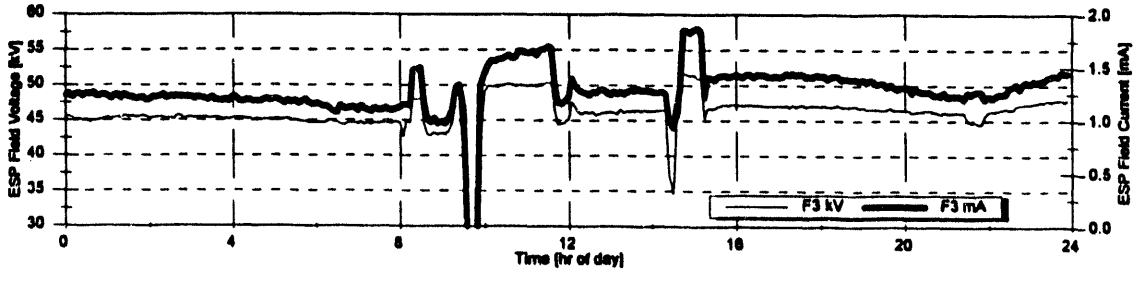

Plate Mass

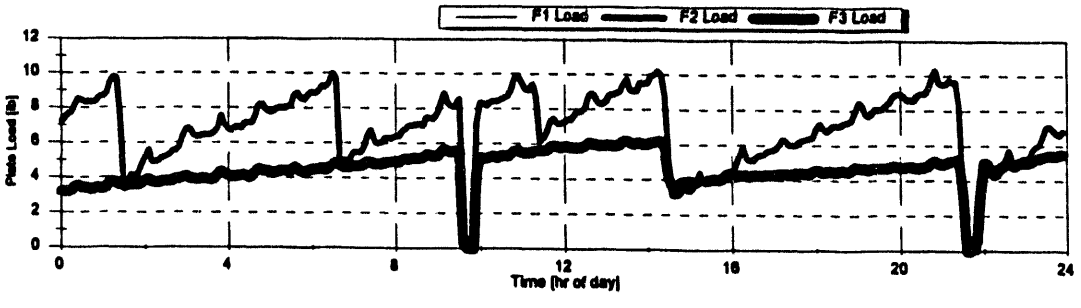

Test Conditions

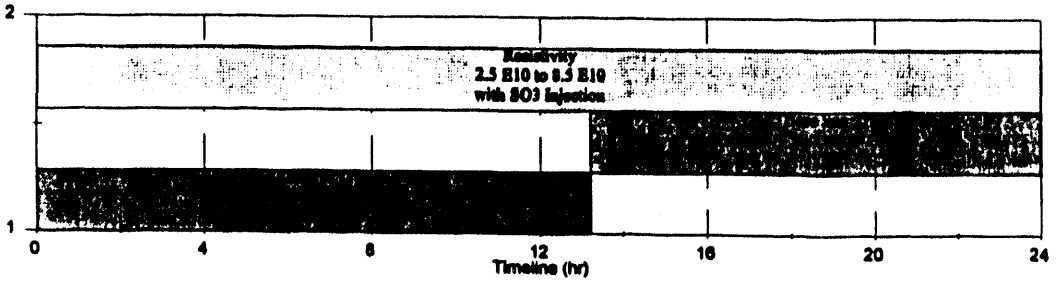

Figure A.7: 09/30/93 ESP Data

Outlet Opacity

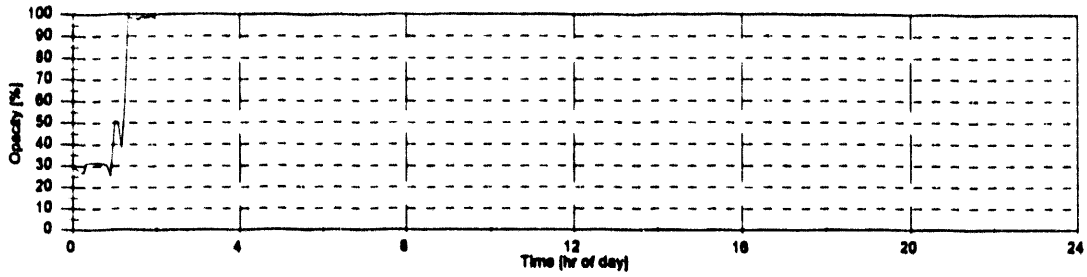

Field 1 Voltage & Current

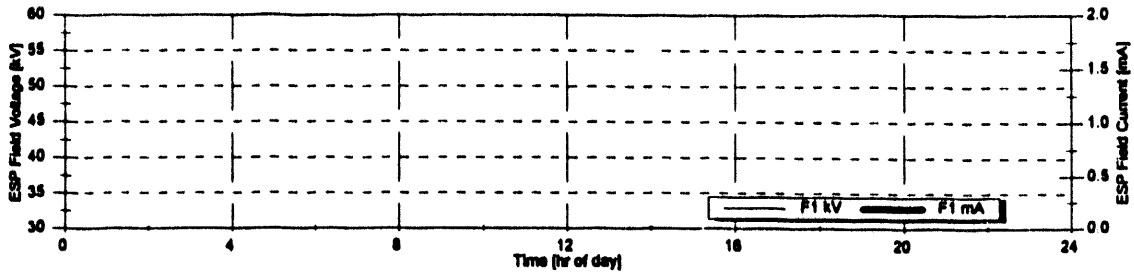

Field 2 Voltage & Current

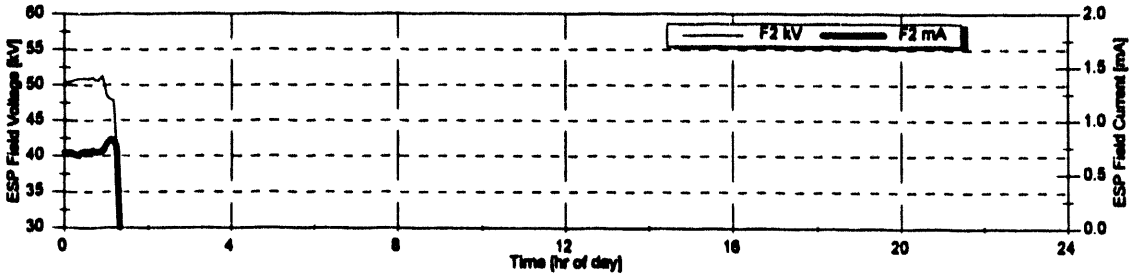

Field 3 Voltage & Current

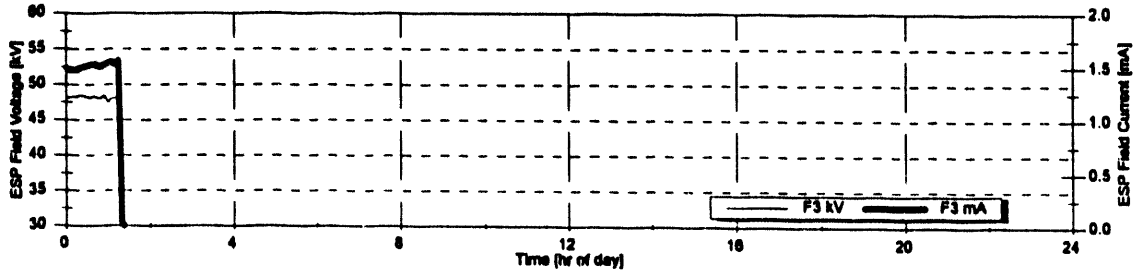

Plate Mass

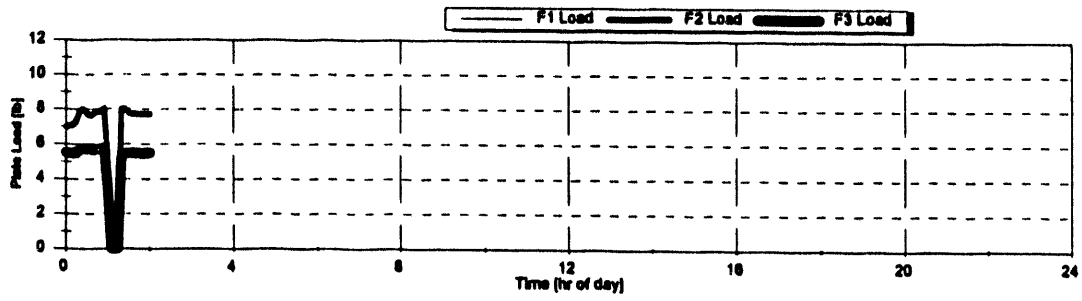

Test Conditions

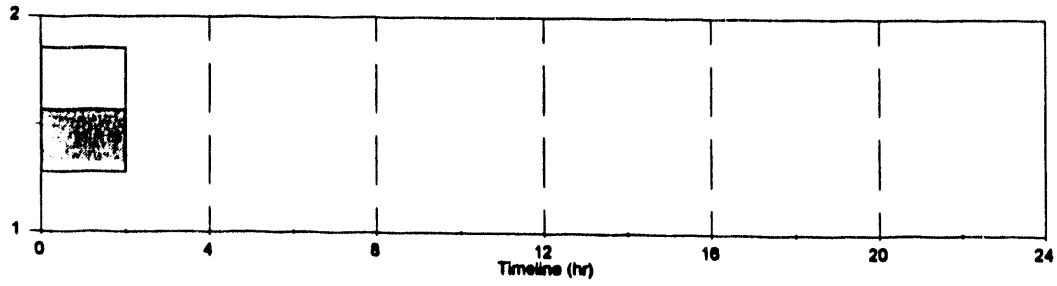

Figure A.8: 10/01/93 ESP Data

Appendix B

Particulate Test Summary

PARTICULATE TEST SUMMARY

Test Number	Test Date	Test Time	Test Condition	Flow (acfm)	Flow (dscfm)	Velocity (ft/sec)	H20 (%)	Stk Temp (oF)	Isokinetic (%)	Mass Concentration (gr/acf)	Mass Concentration (gr/dscf)	Mass Concentration (gm/NM3)	Mass Emission (lbs/hr)	Mass Emission (lbs/mmbtu)
TH2	09/21/93	2217 - 2257	Baseline	467	296	22.3	7.0	288	92.1	0.439	0.691	1.582	1.757	1.194
TH3	09/22/93	1352 - 1452	Baseline	467	296	22.3	7.1	291	90.9	0.400	0.630	1.442	1.601	1.088
TH4	09/22/93	2113 - 2213	Baseline	471	290	22.5	9.1	299	92.7	0.379	0.616	1.411	1.532	1.065
Inlet Baseline Average				468	294	22.4	7.7	293	91.9	0.406	0.646	1.478	1.630	1.116
MF1	09/21/93	2137 - 2307	Baseline	508	322	24.3	7.4	285	94.7	0.005	0.008	0.017	0.021	0.014
MF2	09/21/93	1347 - 1447	Baseline	516	345	24.6	6.6	258	93.6	0.005	0.007	0.017	0.021	0.014
MF3	09/22/93	2120 - 2220	Baseline	515	345	24.6	6.6	255	94.5	0.003	0.005	0.011	0.014	0.009
Outlet Baseline Average (3 fields)				513	337	24.5	6.9	266	94.3	0.004	0.006	0.015	0.019	0.012
TH5	09/28/93	2154 - 2224	Baseline/SO3	493	303	23.5	8.4	301	95.7	0.356	0.580	1.327	1.504	0.950
TH6	09/28/93	2311 - 2342	Baseline/SO3	490	309	23.4	6.0	300	93.0	0.398	0.631	1.444	1.673	1.034
TH7	09/29/93	0029 - 0059	Baseline/SO3	491	309	23.4	6.1	301	94.5	0.426	0.677	1.549	1.790	1.110
Inlet Baseline with SO3 Average				491	307	23.5	6.8	301	94.4	0.393	0.629	1.440	1.656	1.031
MF4	09/28/93	2148 - 2218	Baseline/SO3	526	349	25.1	7.2	252	99.5	0.025	0.037	0.085	0.111	0.069
MF5	09/28/93	2310 - 2340	Baseline/SO3	527	350	25.2	6.4	257	96.7	0.026	0.040	0.090	0.119	0.073
MF6	09/29/93	0027 - 0057	Baseline/SO3	526	354	25.1	5.3	257	93.6	0.028	0.041	0.095	0.125	0.077
Outlet Baseline with SO3 Average (2 fields)				526	351	25.1	6.3	255	96.6	0.026	0.039	0.090	0.118	0.073
TH8	09/29/93	1247 - 1317	Additive C/SO3	501	314	23.9	7.4	299	94.1	0.385	0.615	1.407	1.653	1.007
TH9 *	09/29/93	1359 - 1429	Additive C/SO3	501	316	23.9	6.3	301	95.1	0.127	0.210	0.482	0.476	0.345
TH10	09/29/93	1513 - 1543	Additive C/SO3	498	316	23.8	7.1	290	98.5	0.347	0.546	1.249	1.479	0.894
Inlet Additive 'C' Average			Additive C/SO3	500	315	23.9	7.3	295	96.3	0.366	0.580	1.328	1.566	0.951
MF7	09/29/93	1245 - 1315	Additive C/SO3	525	353	25.1	6.1	256	99.2	0.029	0.043	0.097	0.128	0.079
MF8	09/29/93	1358 - 1428	Additive C/SO3	524	352	25.0	6.3	254	98.0	0.035	0.051	0.118	0.155	0.095
MF9	09/29/93	1512 - 1542	Additive C/SO3	532	359	25.4	6.2	253	96.2	0.028	0.042	0.096	0.129	0.077
Outlet Additive 'C' Average (2 fields)				527	355	25.2	6.2	254	97.8	0.030	0.045	0.104	0.137	0.084
TH11	09/30/93	0850 - 0921	Additive D/SO3	489	309	23.4	6.5	301	97.7	0.331	0.525	1.202	1.390	0.860
TH12	09/30/93	1048 - 1118	Additive D/SO3	487	310	23.3	6.6	294	97.6	0.439	0.691	1.580	1.833	1.131
TH13 *	09/30/93	1156 - 1226	Additive D/SO3	487	308	23.3	7.3	292	95.1	0.149	0.236	0.540	0.623	0.386
Inlet Additive 'D' Average				488	309	23.3	6.5	298	97.6	0.385	0.608	1.391	1.611	0.996
MF10	09/30/93	0851 - 0921	Additive D/SO3	532	359	25.4	6.3	252	97.7	0.030	0.045	0.102	0.137	0.082
MF11	09/30/93	1044 - 1114	Additive D/SO3	530	362	25.3	5.5	250	96.0	0.033	0.048	0.110	0.149	0.089
MF12	09/30/93	1155 - 1225	Additive D/SO3	531	361	25.3	5.6	250	96.1	0.032	0.047	0.108	0.147	0.088
Outlet Additive 'D' Average (2 fields)				531	361	25.4	5.8	251	96.6	0.032	0.047	0.107	0.144	0.086

* Sample results invalidated; excluded from test average.

DATE
FILMED
5/23/94

END